

Université du Québec à Chicoutimi

Mémoire présenté à  
L'Université du Québec à Chicoutimi  
comme exigence partielle  
de la maîtrise en informatique

offerte à

L'Université du Québec à Chicoutimi  
en vertu d'un protocole d'entente  
avec l'Université du Québec à Montréal

par

WANG HaiYan

**Data of Scanned Points' Pre-process and Curved Surface's Reconstruction**

May 2009



### Mise en garde/Advice

Afin de rendre accessible au plus grand nombre le résultat des travaux de recherche menés par ses étudiants gradués et dans l'esprit des règles qui régissent le dépôt et la diffusion des mémoires et thèses produits dans cette Institution, **l'Université du Québec à Chicoutimi (UQAC)** est fière de rendre accessible une version complète et gratuite de cette œuvre.

Motivated by a desire to make the results of its graduate students' research accessible to all, and in accordance with the rules governing the acceptance and diffusion of dissertations and theses in this Institution, the **Université du Québec à Chicoutimi (UQAC)** is proud to make a complete version of this work available at no cost to the reader.

L'auteur conserve néanmoins la propriété du droit d'auteur qui protège ce mémoire ou cette thèse. Ni le mémoire ou la thèse ni des extraits substantiels de ceux-ci ne peuvent être imprimés ou autrement reproduits sans son autorisation.

The author retains ownership of the copyright of this dissertation or thesis. Neither the dissertation or thesis, nor substantial extracts from it, may be printed or otherwise reproduced without the author's permission.

## ACKNOWLEDGEMENT

This thesis would not have been completed without Professor Cao Zuoliang's guide and concern. His precision, knowledge, and scientific working methods and experiences impressed me deeply. Here, I want to express my sincere gratitude to him for his guide and care for my life.

High tributes are also paid to Professor Li Jun for his enthusiastic help and Professor Zhang Baofeng for his suggestion; Also those classmates represented by Lin Yibin who contributed a lot to my thesis; and those experts and teachers who read my thesis and gave me valuable suggestions in their spare time.

Thanks are given to my parents and my family. Their concern, support and encouragement enabled me to finish this thesis.

Thank all the teachers, classmates and friends who helped me and supported me.

## TABLE OF CONTENTS

|  |      |
|--|------|
| <b>ACKNOWLEDGEMENT</b> .....   | i    |
| <b>TABLE OF CONTENTS</b> .....   | ii   |
| <b>LIST OF FIGURES</b> .....   | v    |
| <b>LIST OF TABLES</b> .....  | viii |
| <b>ABSTRACT</b> .....  | ix   |
| <b>CHAPTER 1 INTRODUCTION</b> .....  | i    |
| 1.1 The Application of Color 3D Data Processing Technology .....                         | 3    |
| 1.2 Current Study of 3D Data Processing Technology.....                                  | 4    |
| 1.2.1 Data preprocess .....  | 5    |
| 1.2.2 Curved surface reconstruction.....   | 6    |
| 1.2.3 Other processing technologies .....  | 10   |
| 1.2.4 The common 3D data processing software .....                                       | 11   |
| 1.3 Main Tasks of the Subject .....  | 12   |
| <b>CHAPTER 2 SOFTWARE COMPONENTS OF COLOR LASER SCANNING<br/>SYSTEM</b> .....            | 15   |
| 2.1 Mathematic Model Characteristics of Laser Scanning Data .....                        | 17   |
| 2.2 Selections of the Way of Sticking Color Chart.....                                   | 19   |
| 2.3 Laser Scanning Data Processing Procedure .....                                       | 20   |
| 2.4 The Framework of Software .....  | 21   |
| 2.5 Chapter Summary.....   | 23   |
| <b>CHAPTER 3 THE PRE-PROCESSING OF COLOR LASER SCANNING DATA</b> ..                      | 24   |
| 3.1 Deleting Redundant Data .....  | 25   |
| 3.2 Noise Data Deletion .....  | 31   |
| 3.2.1 Noise data deletion by system judgment.....  | 32   |
| 3.2.2 Point clouds data smoothing algorithm .....  | 33   |
| 3.3 Data Simplification Algorithm .....  | 35   |
| 3.3.1 Factor algorithm .....   | 35   |
| 3.3.2 Spatial algorithm .....  | 36   |
| 3.3.3 Height decision algorithm .....  | 37   |
| 3.3.4 Chord algorithm .....  | 38   |
| 3.3.5 Grid algorithm.....  | 41   |
| 3.4 Adjustment of Simplification Algorithm Under the Restriction of Color Boundary ..... | 44   |

|  |            |
|--|------------|
| 3.4.1 Adjustment of data simplification algorithm under the restriction of color-boundary .... | 45         |
| 3.4.2 The revision of simplification algorithm.....  | 47         |
| 3.5 Chapter Summary.....   | 49         |
| <b>CHAPTER 4 COLOR CURVED SURFACE RECONSTRUCTION .....</b>                                     | <b>50</b>  |
| 4.1 The Fitting of Free Curves And Curved Surface.....   | 52         |
| 4.1.1 Free curve mathematic model .....  | 52         |
| 4.1.2 Free curved surface reconstruction.....  | 60         |
| 4.1.3 B-Spline curved surface smoothing algorithm .....  | 62         |
| 4.2 Mesh Reconstruction.....   | 63         |
| 4.2.1 Scanning data triangular meshing .....   | 64         |
| 4.2.2 The Realization Of Triangular Mesh Data Structure.....                                   | 67         |
| 4.3 Mesh Smoothing Algorithm.....  | 70         |
| 4.3.1 Laplace smoothing algorithm.....   | 71         |
| 4.3.2 Taubin smoothing algorithm <sup>[17]</sup> .....   | 73         |
| 4.3.3 Desbrun algorithm <sup>[46]</sup> .....  | 74         |
| 4.3.4 Mesh subdivision algorithm <sup>[18]</sup> .....   | 76         |
| 4.4 Mesh Simplification .....  | 78         |
| 4.5 Chapter Summary.....   | 82         |
| <b>CHAPTER 5 3D DISPLAYING TECHNOLOGY AND APPLICATION</b>                                      |            |
| <b>INTERFACE.....</b>  | <b>83</b>  |
| 5.1 A Brief Introduction of OpenGL Function.....   | 84         |
| 5.2 The Realization of Key Operations In Displaying .....                                      | 85         |
| 5.2.1 Field range adjustment .....   | 86         |
| 5.2.2 Mouse control.....   | 89         |
| 5.2.3 Mutual transformation of world coordinate and screen coordinate.....                     | 90         |
| 5.2.4 Three-dimension quality and sense of reality displaying .....                            | 92         |
| 5.2.5 Methods to display efficiently.....  | 94         |
| 5.3 Data exchanging of application interface.....  | 96         |
| 5.3.1 ASC .....  | 96         |
| 5.3.2 STL.....   | 97         |
| 5.3.3 IGES.....  | 98         |
| 5.3.4 DXF.....   | 99         |
| 5.3.5 Examples of algorithm implementation .....   | 100        |
| 5.4 Chapter Summary.....   | 101        |
| <b>CHAPTER 6 INTRODUCTION OF SOFTWARE AND PROCESSING</b>                                       |            |
| <b>EXAMPLES OF COLOR SCANNING DATA .....</b>   | <b>102</b> |

|  |  |            |
|--|--|------------|
| 6.1  | Introduction Of Software .....                         | 103        |
| 6.1.1  | Display setting.....                                   | 105        |
| 6.1.2  | Graph input and output.....                            | 106        |
| 6.1.3  | Data processing .....                                  | 106        |
| 6.2  | The Processing of Pencil-Sharpener Scanning Data ..... | 107        |
| 6.3  | Chapter Summary.....                                   | 110        |
| <b>CHAPTER 7 CONCLUSION AND EXPECTATION.....</b> |  | <b>112</b> |
| <b>BIBLIOGRAPHIES .....</b>                      |  | <b>116</b> |

## LIST OF FIGURES

|   |    |
|---|----|
| Figure 1.1 Reverse engineering procedure.....   | 3  |
| Figure 2.1 Rough sketch of laser scanning system.....   | 17 |
| Figure 2.2 The arranging characteristics of the coordinate system and scanning lines of the scanning system ..... | 18 |
| Figure 2.3 The general procedure of laser scanning data processing.....   | 20 |
| Figure 2.4 The framework of the software.....   | 22 |
| Figure 3.1 Flow of frame selection to delete point data.....  | 26 |
| Figure 3.2 Calculation of 2D vector cross product .....   | 27 |
| Figure 3.3 Judge the shape of polygon .....   | 28 |
| Figure 3.4 The method of acreage.....   | 29 |
| Figure 3.5 Method of vector sequence cross product .....  | 30 |
| Figure 3.6 The effect of polygon frame-selection algorithm .....  | 31 |
| Figure 3.7 The description of points position information.....  | 33 |
| Figure 3.8 Point data smoothing algorithm.....  | 35 |
| Figure 3.9 Effect of median algorithm processing.....   | 35 |
| Figure 3.10 Height Decision algorithm diagram .....   | 37 |
| Figure 3.11 Chordal algorithm diagram.....  | 39 |
| Figure 3.12 Chordal algorithm procedure.....  | 40 |
| Figure 3.13 The diagram of grid algorithm processing.....   | 41 |
| Figure 3.14 Influences of color boundary on the restruction of color model.....                                   | 45 |
| Figure 3.15 RGB color space.....  | 46 |
| Figure 3.16 Procedure of grid simplification algorithm of color boundary .....                                    | 48 |

|  |     |
|--|-----|
| Figure 4.1 B-Spline curved surface diagram.....                            | 61  |
| Figure 4.2 Effect by B-Spline smoothing algorithm.....                     | 62  |
| Figure 4.3 Triangular mesh reconstruction rough sketch.....                | 65  |
| Figure 4.4 Direction vector calculation rough sketch .....                 | 66  |
| Figure 4.5 Halfedge structural representation .....                        | 68  |
| Figure 4.6 Laplace and Desbrun' smoothing algorithms diagram.....          | 72  |
| Figure 4.7 Taubin's filtering function .....                               | 73  |
| Figure 4.8 Effect of mesh smoothing algorithms.....                        | 76  |
| Figure 4.9 Relationship between new mesh vertexes and boundary points..... | 77  |
| Figure 4.10 Edge contraction diagram.....                                  | 80  |
| Figure 4.11 Mesh subdivision effect.....                                   | 81  |
| Figure 4.12 Mesh reduction effect .....                                    | 81  |
| Figure 4.13 The processing effect of flowerpot solid.....                  | 82  |
| Figure 5.1 OpenGL displaying processing procedures.....                    | 86  |
| Figure 5.2 World coordinates and view point coordinates.....               | 87  |
| Figure 5.3 Perspective projection sketch map.....                          | 89  |
| Figure 5.4 Effect of field range adjustment.....                           | 89  |
| Figure 5.5 Influences of illumination on field displaying .....            | 93  |
| Figure 5.6 Examples for the format of application files.....               | 97  |
| Figure 5.7 IGES File Structure .....                                       | 98  |
| Figure 5.8 Procedure of reading and calculating ASC files .....            | 101 |
| Figure 6.1 Using scanning system to get the 3D data of object .....        | 104 |
| Figure 6.2 Original point clouds of a ball surface.....                    | 105 |
| Figure 6.3 Coordinate scale setting of axis x.....                         | 106 |
| Figure 6.4 Real image to be processed.....                                 | 107 |

|   |     |
|---|-----|
| Figure 6.5 Original point clouds (68961points ) ..... | 108 |
| Figure 6.6 Process of noise deletion.....             | 108 |
| Figure 6.7 Noise deletion result (68551points) .....  | 109 |
| Figure 6.8 Point clouds simplification.....           | 110 |
| Figure 6.9 Color model.....                           | 110 |

## LIST OF TABLES

|   |    |
|---|----|
| Table 3.1 Effect of the various simplification algorithms.....                    | 43 |
| Table 3.2 Comparative table of color scanning line simplification .....           | 47 |
| Table 4.1 The influence of CPN on fitting precision and smoothing degree.....     | 58 |
| Table 4.2 Characteristics Comparison of the common mesh smoothing algorithms..... | 75 |

## ABSTRACT

Basing on the whole processing of color three-dimensional model laser scanning data, the algorithms and software development was analyzed and researched. The whole procedure includes two parts. One is the pre-processing of point clouds and the other is surface reconstruction. It is the main purpose of this thesis to establish the color three-dimensional model and implement the data interface with other applications. The purpose has been achieved partly, and the software for processing is designed at the same time, which has the standard interface with the laser scanning system. So the processing system and software can be applied in the manufacturing and virtual reality technique, such as the network museum.

The main research work of this thesis is:

1. The main procedure and key algorithms of the pre-processing for color three-dimensional model point clouds has been analyzed, and the integrated method of system judgment and manual selection is used to delete the noise data effectively (Chapter 2).

2. The point clouds data reduction algorithm with the color-boundary preservation in RGB color space is proposed in this paper. The algorithm can avoid both the shape and color distortion (Chapter 3).

3. The smoothing algorithm based on the B-Spline surface fitting is implemented. It is proved by the theory and experiments that this smoothing algorithm has the favorably controllable ability (Chapter 3).

4. In the processing of color surface reconstruction, the mesh algorithm is implemented using the half-edge structure. And it can realize easily the post processing, such as mesh smoothing and mesh reduction (Chapter 4).

5. The key problems on the display of color model in the OpenGL platform are solved (Chapter 5). The robust processing software, 3D Color Surf Ver1.0, is developed using C++ language. The framework is layered, that fulfills the function partition lightly. So the software can be revised and updated flexibly (Chapter 6).

**CHAPTER 1**  
**INTRODUCTION**

# CHAPTER 1

## INTRODUCTION

Digital models are used in a wide range of applications including architectural visualization, prototyping in Computer-Aided Manufacturing (CAM), scientific simulations, and digital characters and environments for the entertainment industry. Thus, there is tremendous demand for a wide variety of digital models and the tools to construct and edit them. Non-touching three-dimensional model data acquiring technology, especially laser scanning technology has been significant progress in quick measuring and easy operating. These techniques can acquire a lot of digital data points of the model. Monochrome three-dimensional (3D) model data processing had long been the key subject of the scientists. However, the digitalization of color three-dimensional models and data processing systems is called for in many areas. How to acquire the color three-dimensional model data, realize the preprocessing of the digital data, construct digital model and display so on? This dissertation aims to study the above problems from the aspect of three-dimensional model data processing.

## 1.1 The Application of Color 3D Data Processing Technology

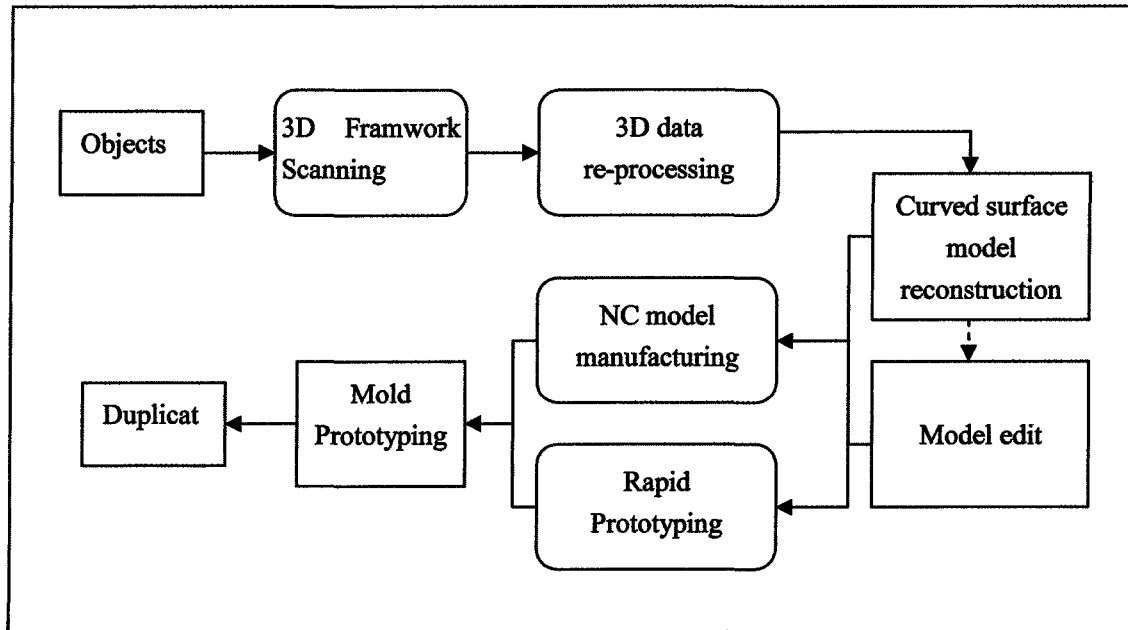


**Figure 1.1** Reverse engineering procedure

The processed and reconstructed 3D data can be applied in CAD, CAM, RE and RP (Rapid Prototyping). The objects accumulated and constructed by 3D data transforms into CAD model, which can be directly used in computer numerical control (CNC) and be duplicated or be twice designed and developed. This process is what we call reverse engineering, which saved the time and cost in model development. Figure 1.1 shows its procedure. Adding color applications to this technology can improve the additional value of the system and the product, especially when it is used in the processing of toys and the outer shells of family electronic properties.

VRML, as the production of network and virtual reality technology, has developed

rapidly in the recent years. It can make people browse the colorful 3D fields everywhere in the world on network. Color 3D data processing technology can realize the 3D digitalization of tools, antiques and the other merchandises, produce lively substantial solid color model and speed up the application of virtual reality technology in cyber games, network museums and cyber shopping, etc.

In the recent years, 3D data reconstruction and the prototyping technology have also been applied in medical areas such as snaggletooth diorthosis and skull recovery. Meanwhile, the constructed color 3D model information can also directly contributes to the security identification of national defense departments, legal enforcement institutions and government organs.

## **1.2 Current Study of 3D Data Processing Technology**

The technology of 3D data processing is a whole new field to me. A lot of time is spent to study the relative knowledge of it. The technology of 3D data measurement is one of the most important procedures in the whole processing, and 3D points data can be acquired by scanning before processing.

The ways of 3D data measuring mainly contains two kinds: non-touching and touching. The representative of touching way is three-coordinate measuring machine. It has the characteristics of high precision, slow speed and unsuitableness to measure the soft and easily-cut objects. Non-touching includes: laser visual measuring <sup>[1]</sup> and strip visual

measuring method [21]. They are easy to be operated and measure quickly, which can be used in rather condense objects. 3D data organizing forms derived from different measuring methods are different, and they can be roughly divided into orderly points and scattering points data, which are figuratively called point clouds data. For different forms of data points, the processing way and procedure are various.

The reconstructed model has two forms: wire and solid. The wire model is connected by linking line of point clouds data. While the solid interpolates those points which are not caught by scanning and displays the complete digital model of the solid, so it seems real and dimensional. The solid model is the ultimate result of 3D data processing.

The core of 3D data processing technology is: data preprocess and curved surface reconstruction. They are to be introduced as the following.

### **1.2.1 Data preprocess**

The principle of data preprocess is to reduce enormous data and smooth it in the premise of not influencing the precision of reconstructed curved surface. The procedures can be divided as the rearrange the disorderly point clouds data, deleting of noise points, smoothing processing, data simplification and reconstruction [3]. Generally speaking, laser scanning data arranges orderly according to the rules, so the pre-process and reconstruction are relatively easy. So although scatted point clouds data has its own procedure of processing, it is still an effective way to process it according to that of orderly point clouds

data after reorganizing. Bibliography [4] realized the sequence arrangement of the scattered point clouds data based on the criterion of vector angle.

For those enormous point clouds data, the key of preprocessing is focused on the study of data simplification algorithm. The simplified data can save storage space and reduce the time consumed in reconstructing and displaying. By sampling point clouds data, simplified data can be acquired, but it can not avoid distortion in appearance of the objects. While with the definition of chord length proposed by Rogers and Adams as a criterion[5], both data simplification and the appearance of the objects can be achieved. Some people represented by K.H.Lee proposed the concept of curvature angle [6] and based on the value of it, they precede partition and simplification by grids. Grid has the variation of two-dimensional (2D) and three-dimensional (3D) grids. The latter surpassed 2D in the judgment of deepness and improves the credibility in data simplification. Aiming at Color 3D data processing [7], this thesis takes color boundary restriction into consideration and avoids the color distortion after model reconstruction.

### **1.2.2 Curved surface reconstruction**

Curved surface reconstruction is to build solid math model, which is proposed firstly by Hoppe in 1992 in his bibliography, see [8]. And many other bibliographies carried out thorough studies and proposed many methods after him. The common ones are listed below:

## 1 . Free curved surface reconstruction

The theory is based on the free curves, curved surface model proposed by Bezier in the 1970's, especially the B-Spline and NURBS theories which have now become one of the mathematic criterion in describing industry products. In bibliography [9], Pigel and Tiller proposed the method of approximating scattered point clouds data with B-Spline curved surface and constructing the matrix-distributed data into smooth continuum curved surface; Forsey and Bartels proposed B-Spline [10] to reconstruct and edit the curved surface with a multi-level mesh, making it more and more delicate and close to point clouds data; later, Lees Wolberg proposed multi-level B-Spline interpolation[11], seeking the answer of a group of references points through solving an indefinite equation, thus implements the overall polishing of the curved surface. By using the algorithm of curved surface reconstruction, we can easily get random continuum curved surface model, but it needs a lot of calculations and patience as well as the matrix-scattered point clouds data structure, so the application has certain limitation.

## 2 . Mesh reconstruction

Mesh reconstruction algorithm is widely used recently due to its rapid model reconstruction of mass point clouds data and its accordance with industry and computer display. The chart Vorono can be directly used on the scattered points and carry on Delaunay triangular [12]. The criterion is the principle of the biggest angle the least

proposed by Lawson [13]. This principle can be conveniently used in the reconstruction of laser scanning data and the mesh reconstruction of the model. Bradley, in his bibliography (see [14]) put forward a mesh curved surface reconstruction algorithm which is increased with the rising of seed points. Started from the selected seed points, this algorithm judges whether the selected points is on the mesh and their relationship through the visible relationship between the candidate points and the current mesh, which ultimately gets one or more mesh surface as the reconstructed one. Floater proposed the meshless parameter curved surface algorithm [15], which firstly projects the original point clouds data on the platform and then joins these projection points into a triangle mesh directed by Delaunay's plane method of triangularization. Based on this relationship, the mesh reconstruction curved surface of the original point clouds data can be created.

But mesh reconstruction curved surface can only achieve  $C^0$  continuum, so in order to get smooth model, we need to do some smoothing process after reconstruction as well as acquiring better pre-processing data. C. Zeng and M. Sonka used low pass filter to preserve smoothing[16]; G. Taubin improved Gaussian's smoothing algorithm; Some other investigators started from the other aspect, who subdivides the mesh and improved the smoothing degree of the model [17], B. Wyvill Bezier fitted the curved surface on the brink of the mesh and subdivided the mesh by interpolating some control points[18]; P. Volino and N. M. Thalmann in bibliography [19], used directly the normal vector in triangle mesh

and in the vector normal to divide points, which is an easy and effective way.

Mesh model usually consists of ten thousands of, even millions of polygon faces. The over-huge solid mesh models are usually unwieldy for the direct ratio relationship between the molding time and the number of the polygons. And on the other hand, in virtual reality, sometimes it is unnecessary to display the model in detail, so we can construct some models in LOD (Level of Detail) for each object, and choose the suitable one. In order to satisfy the requirement of analyzing, displaying and storing in computer, Simplification or Compression of the model should be carried on. William, in bibliography[20], proposed a method to achieve the aim. Firstly judge the distance of the average plane formed by the points and the territory point, and then delete the point with a shorter distance value than valve, and grid the points again which are near the hole, thus simplify the mesh; While P. Verson and some others proposed to decide whether the vertex should be deleted by curvature and error measurements [21]. Rossignac and Borrel break the original model into blocks, and replace each point in the congeries with another point, and then remesh these vertexes. This method has the characteristics of quick algorithm, simplified data, but the weakness is that the effect of the display is not satisfying [22]. In contrast, the studies on Iterative edge contraction are in circulation. While guarantee the invariableness of the original point clouds data and change only the topology structure of the points, it is easy to realize the dynamic display in different distinction ratio.

Bibliographies [23, 24] are examples of this algorithm, which simplified mesh through contracting the edge shorter than valve value into one point based on some error metric. The difference between various algorithms lies in the different selection of error standard. The most famous one is Garland's simplification algorithm [23]. And some bibliographies put forward the simplification algorithm of maintaining the property of model, such as the color and the stripe [25].

### 3 . Other methods

There are still many other methods, Zhao and some others put forward a minimal-surface-like mode and PDE partial differential equation in [26], known as implicit curved surface reconstruction. By taking some collection of the original point clouds data as initial curved surface, making it changing continuously toward certain direction of the energetic equation grads, we can obtain reconstructed curved surface. But such implicit curved surface reconstruction methods need the building of complex functions, so it is only suitable for the simple construction. However, in the recent years, with the development of neuron network algorithm, some reconstruction algorithms adopts multi-level sensor[27,28] to acquire the innate mathematical relationship in the free curved surface with precision and speed.

#### 1.2.3 Other processing technologies

The above methods are suitable to the moderate scanning data. As for the

processing of mass data, the above method is not only complicated but also may cause waste in the system sources. So the partition and reconstruction of the data are required, which need partition algorithm of the data. The algorithms consist of partition based on the line and partition based on the curved surface. More effective line partition algorithm is founded on the method of surface curvature detection boundary. Milory introduced the concept of active contour in linking the edge point and increased the stability of curvature detection algorithm <sup>[29]</sup>. The characteristics of Yang M algorithm are that it is precise and effective in calculating curvature by parameter curved surface fitting <sup>[30]</sup>.

As for the huge object, we can not acquire complete point clouds data once and for all due to the influence of the scope of systemic measurement, so we choose to separate the objects into different parts and collect them partly. For either data, the various reconstructed curved surfaces are to be combined with their corresponding patching-up algorithm. The common one is ICP (Iterative Closet Point) <sup>[31]</sup>

#### **1.2.4 The common 3D data processing software**

3D softwares in industry is usually divided into 2 kinds: CAD/CAM design software and 3D reverse engineering software. And the famous 3D design softwares are like AutoCAD, UG, Pro/ENGINEER and SolidEdge. Reverse engineering softwares contain GeoMagic of American company RainDrop, Surfacer of American Imageware , Rapid Form of Korean INUS, etc. 3D data processing software usually refers to the

latter , which can acquire curve and curved surface model in good quality. But in application, these curves and curved surfaces data should be transformed into the present CAD/CAM system in standard point forms, so they always act as the third party software of CAD/CAM design software. Generally, the well- known reverse engineering software is multi-functional and usually be imported abroad and be expensive. Although, there are some studies in our country, for example, the study of Tsinghua university, Chekiang university, Nanking university of aviation and spaceflight, still there are some defects in function and stability. Besides, the common 3D processing software has the all-purpose function, so it is imperfect in some definite data processing, for example, the special color 3D data processing software is still rare.

### **1.3 Main Tasks of the Subject**

This thesis analyses the structure characteristics of laser scanning color data, and studies the corresponding processing method based on the data characteristics. The process consists of two parts: point clouds data pre-process and curved surface reconstruction. Combining the color attributes of the data, the thesis defines the corresponding color boundary restriction in algorithm and revises the point clouds data simplification algorithm. And studies on reconstructed model's mesh smoothing and simplification algorithm are also carried out. In Visual C++ compiling environment and OpenGL environment, the software design of processing algorithm and a whole set of relative perfect software system

are implemented. And it also analyzes the important interface file format in color 3D reconstruction and provides the interface function for reverse engineering technology and the common-used 3D software (AutoCAD).

Main contents of the study :

- 1 . Two procedure of processing color 3D laser scanning data: point clouds pre-process and color model reconstruction.
- 2 . The integrated method of system judgment and manual selection is used to delete the noise data and eliminate the random errors in corresponding smoothing algorithm; the point clouds data simplification algorithm combining with the color-boundary preservation in RGB color space is proposed. The algorithm can avoid distortion both in shape and in color.
- 3 . In the process of curved surface reconstruction, the mesh algorithm is implemented, and it can realize easily the post processing, such as mesh smoothing and mesh simplification. And the thesis also analyzes the B-Spline free curved surface reconstruction algorithm. This smoothing algorithm has favorable controllable ability.
- 4 . The file format of the application interface is analyzed and the data exchanging interface are provided for AutoCAD and reverse engineering (CNC machine).
- 5 . The design and programming of processing software are fulfilled with C++

language. The framework is layered which brings about the separation of algorithm and data. And the function partition guaranteed the flexibility of the software.

- 6 . The key problems of OpenGL platform environment setting are analyzed. And the problems of how to realize the scene adjustments of data, maintain human-computer interaction and the model's likeliness and precise display are discussed.

**CHAPTER 2**  
**SOFTWARE COMPONENTS OF COLOR LASER**  
**SCANNING SYSTEM**

## **CHAPTER 2**

### **SOFTWARE COMPONENTS OF 3D COLOR LASER SCANNING SYSTEM**

Three-dimensional (3D) laser scanning <sup>[56]</sup> is a non-contact technology that digitally captures the shape of physical objects using laser light. 3D laser scanners create a point cloud of data samples from the surface of the object from which a digital CAD model can be made.

Color laser scanning system is composed of scanning device and data processing software. The scanning device of 3D data contains sensor which is made up by line structured light and sensor of camera by CCD, and the stepper electronic machine which controls the movement of the object. The movement can make the sensor capture the 3D data of the different parts of the object, when it moves according to certain rule, the system can acquire the partial or even the whole surface outline. Those data points are called point clouds data. The digital model of the object can be obtained by corresponding pre-processing and reconstruction of it. And there also accompanies a process of color chart sticking in this reconstruction of color object. Meanwhile, in order to enhance the application of the software, the corresponding application data interface should be provided,

which will realize both the data exchanging with other processing system and can also be used in manufacturing or in virtual reality technology.

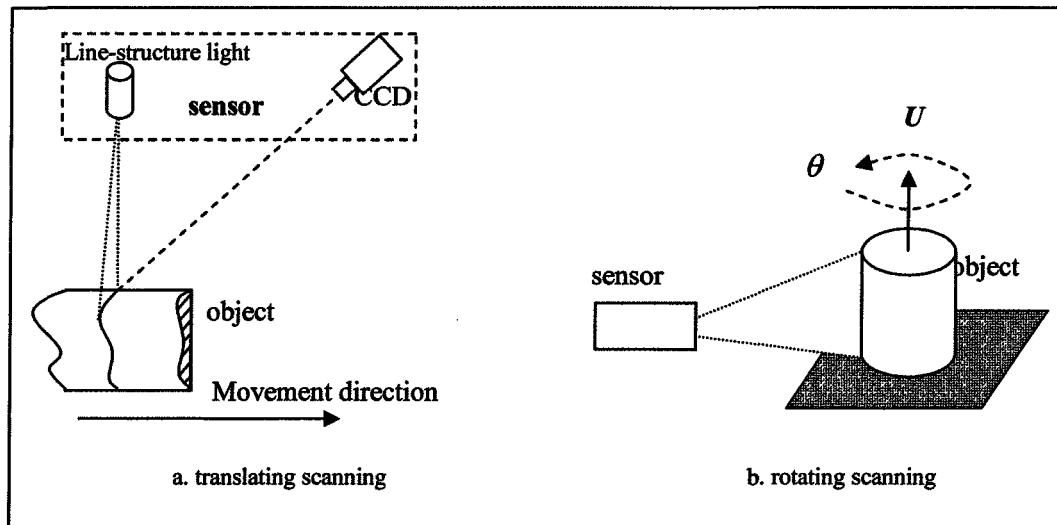
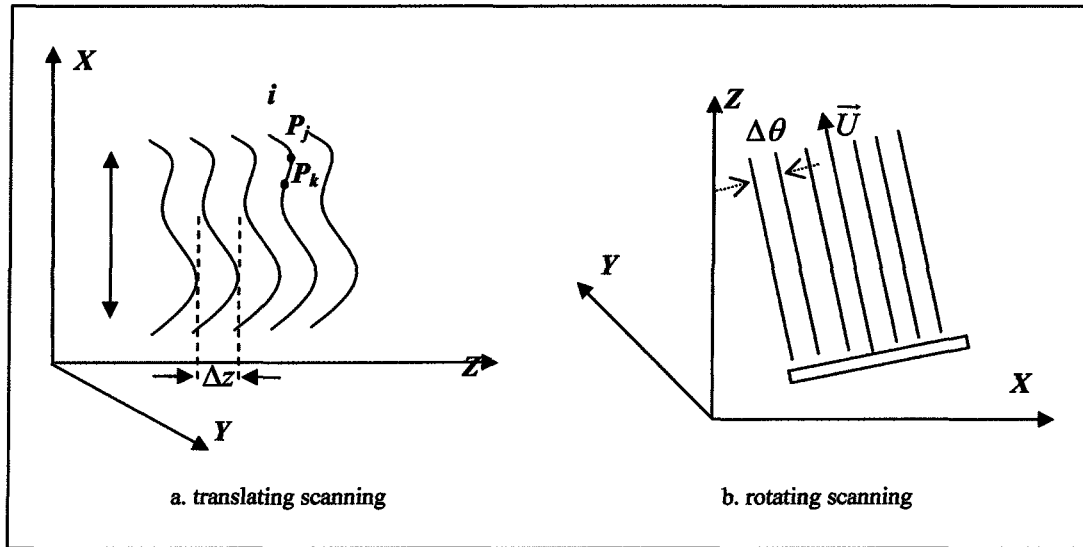


Figure 2.1 Rough sketch of laser scanning system

## 2.1 Mathematic Model Characteristics of Laser Scanning Data

Among the various scanning modes, two kinds can be summarized according to the way of movement of the scanning objects: translating scanning and rotating scanning [32]. Figure 2.1 shows the rough sketch of translating scanning way based on the principle of trigonometry. The sensor collects a series of scanning lines as the objects moves along the normal vector on the light plane. As indicated by Figure 2.2(a), the movement direction of the object is on the axis Z, and the height and deepness of the scanning lines correspond to axis X and Y, which forms the right-hand coordinate system. The distance between the scanning lines is  $\Delta z$  (the object's movement distance), and each point data on the scanning lines has the same Z coordinate value, namely, for the *i*th scanning line, the coordinate

value of  $P_j$  and  $P_k$  can be labeled as  $(x_j, y_j, z_i)$  and  $(x_k, y_k, z_i)$ . And the data value on the axis X is changing according to certain rule. eg. The value relationship on scanning points j and k is  $x_j \geq x_k$ ; And the value on axis Y is determined by the appearance of objects.



**Figure 2.2** The arranging characteristics of the coordinate system and scanning lines of the scanning system

Figure 2.1(b) is the rough chart of the rotating way of scanning. The object revolves around axis  $\bar{U}$ , the stepper angle is  $\Delta\theta$ . Figure 2.2(b) indicates the coordinates creation methods of this scanning way [32]. Firstly, determine the 3D coordinate XYZ, then set the axis  $\bar{U}$  around which the object is revolving, and the revolving angle is  $\Delta\theta$ . Finally, transform those coordinate value into the uniform 3D reference frame XYZ and obtain the 3D coordinate value  $(x, y, z)$ . Due to the uncertain direction of the scanning axis, the acquired Point Clouds data only has the characteristics of sequencing according to the scanning lines instead of arranging translated.

## 2.2 Selections of the Way of Sticking Color Chart

The common seen color chart sticking is isolated form the scanning and processing of 3D data. The usual procedures are: (1) object scanning to acquire the 3D data (2) reconstruct the model (3) collect the object's complete color 2D pictures into each 3D point through projection function to implement the color chart sticking .

As for the color information  $C(u, v)$  of any point  $P(u, v)$  in the plane chart, there are 3 quantums as the following.

$$C(u, v) = (R(u, v), G(u, v), B(u, v)) \quad (2.1)$$

This color information is projected onto the 3D space point  $P(x, y, z)$ . The key of the process is to determine the projection relationship. Bibliography [33] mentioned a method used to project by parted protruding quardrangle. But the scanning object is moving continuously and erracticly, so it is a very complicated process to determine the projection function of 3D point and 2D color data.

In order to avoid the complex projection function in the experiment of the subject, the 3D data color information determined in the scanning process is adopted directly, which is proposed by bibliography [32]. In detail: firstly, under the black-and-white mode of CCD camera, project the line structured light of each position of the object and get the surface geometry information  $(x, y, z)$  ; then transform the camera into color mode and collect the color information 2D  $(R, G, B)$  of the coordinate  $(u, v)$  on the corresponding

computer color pictures. The geometry and color information of each point on laser line combine together and make up the complete color laser scanning data (x, y, z, R, G, B). The complete scanning data can be directly applied in the later processing.

### 2.3 Laser Scanning Data Processing Procedure

There is no fixed procedure in the process of 3D scanning data, the different processes are selected by the requirements. Figure 2.3 shows the common-used process procedure.

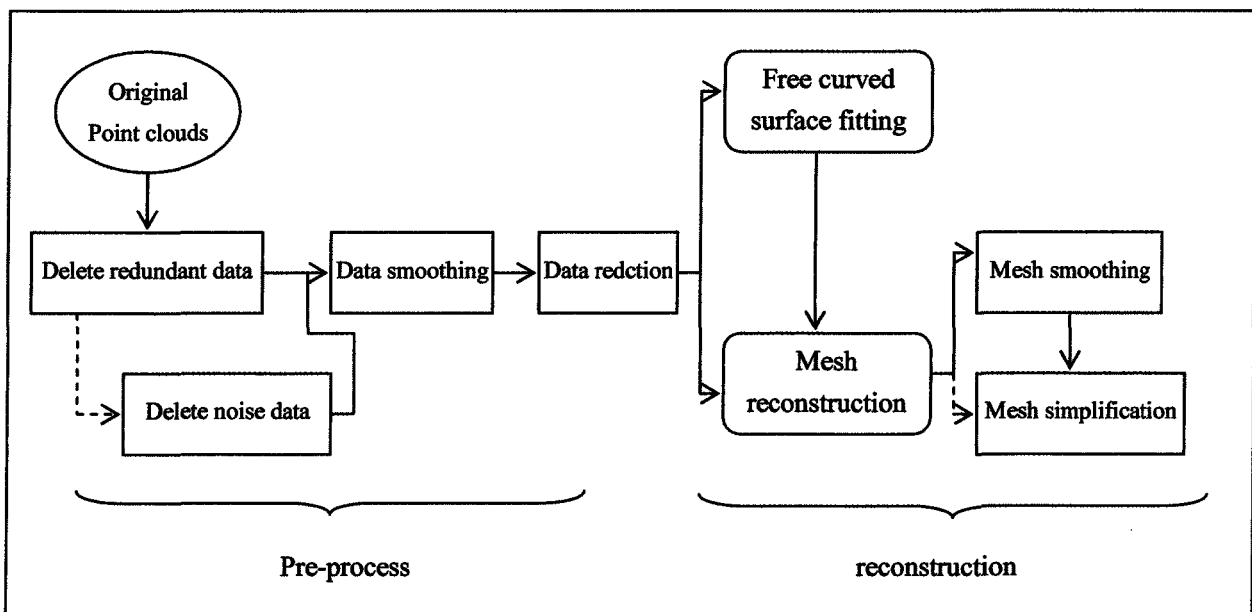


**Figure2.3** The general procedure of laser scanning data processing

The process can be divided into two steps: data pre-process and reconstruction. The tasks of data pre-process are mainly as the following, noise point deleting and data smoothing and simplification which will be presented in chapter 3. In data reconstruction,

the solid model construction and post-processing are required. And the further process algorithm is selected according to the specific traits of the data. For example, in selecting reconstruction algorithm, free curved surface reconstruction algorithm is selected for those objects with simple shapes and regular data points; otherwise, the mesh algorithm reconstruction is more convenient, but this method should be added with smoothing process to achieve satisfactory effect. And there is something special about data process. In the process of reducing point clouds data, the restriction of color-boundary should be paid attention to. Besides, the same problems should be re-emphasized in mesh simplification and partition.

## **2.4 The Framework of Software**

The OpenGL operating environment decides that the software contains not only the necessary processing algorithm but also the function of setting and control of the environment. The whole framework of the processing software is multi-level structured, indicated by Figure 2.4. The OpenGL setting and control level is the bottom platform of the software and undertakes the responsibility of encapsulating the functions of OpenGL, which simplifies greatly the programming and maintaining job of the software and realizes the complete display and control of the scene; the biggest advantage of the hierarchical structure is the realization of the separation of data stratum and algorithm realization stratum. It can conveniently expand various processing algorithms, and improve the

efficiency of graph processing and the feasibility of software updating; and the document interface level provides abundant data interfaces, which guarantees the data exchanging between application environment and the scanning system. Among those, the data is the core of the software, each having the corresponding interface with the other stratum, and implements the feasible displaying and updating coordination of various data.

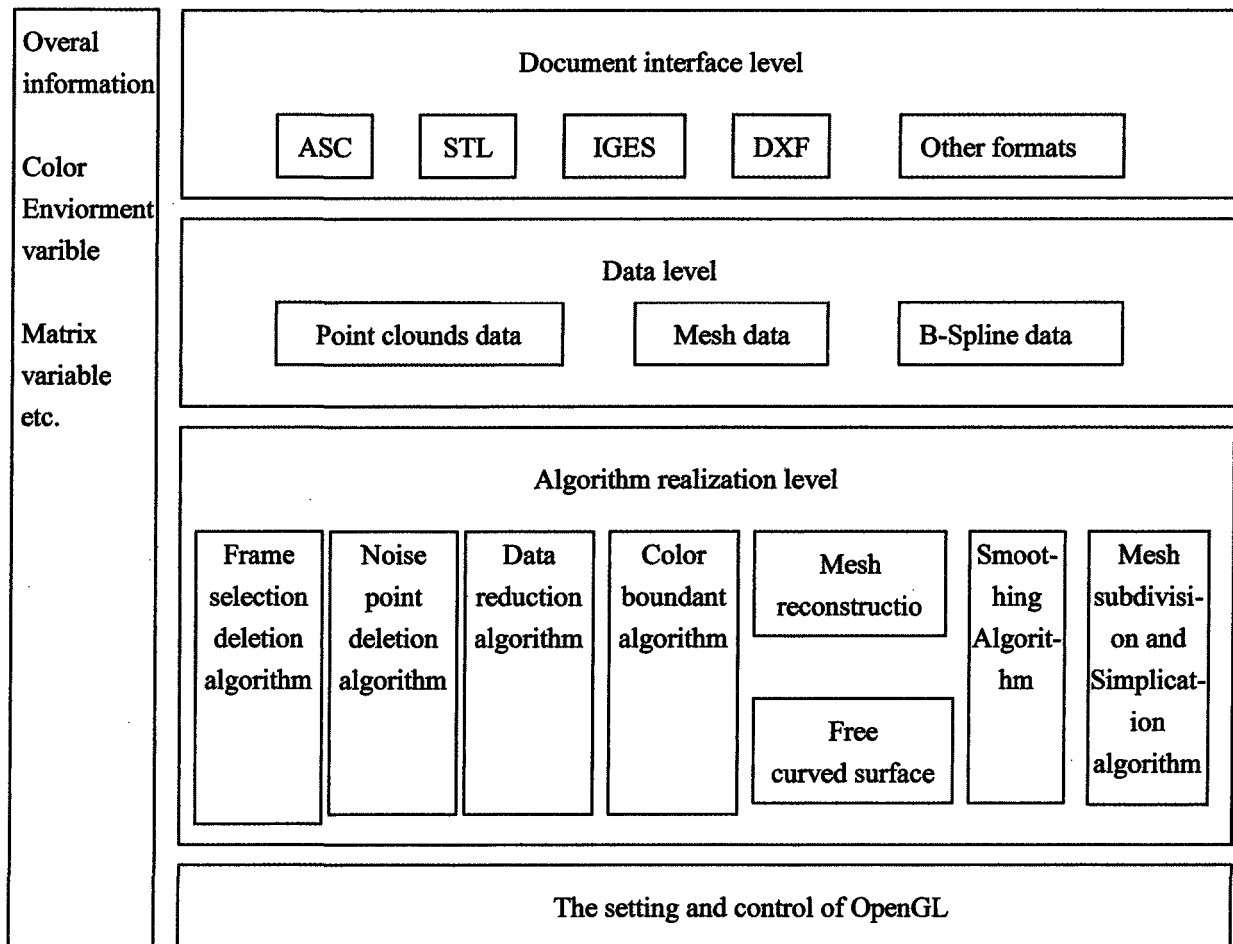


**Figure 2.4** The framework of the software

## **2.5 Chapter Summary**

In this chapter I described the technology of three-dimensional laser scanning system in order to obtain the point cloud of data samples from the surface of the object for the latter processing. The color laser scanning system is composed of scanning device and data processing software. The latter is mainly presented in the components, including the mathematic model characteristics of laser scanning system, the laser scanning data processing procedure and the selections of the way of sticking color chart etc. In the next chapter, the pre-processing of color laser scanning data will be described.

**CHAPTER 3**  
**THE PRE-PROCESSING OF COLOR LASER SCANNING**  
**DATA**

## **CHAPTER 3**

# **THE PRE-PROCESSING OF COLOR LASER SCANNING DATA**

By virtue of enormous data of laser scanning and intensive density of point data, laser line will cast in the visible range of objects not in measurement of CCD such as platform which leads to the phenomenon of redundant data. The scanning data is affected easily by environment and system, which results in disturbing noises. The processing of color laser includes data simplification, smoothing and noise data deletion. The detail process and the sequence of process should be determined by the characteristic of data. Favorable pre-processing will ensure the required accurate point clouds data in the post processing, it can not only improve the accuracy of the post processing but also decline the complexity of the post processing.

### **3.1 Deleting Redundant Data**

The redundant data is obtained from scanning objects lying on the platform is absolutely random, so manual method is implemented by combining the appearance of scanning object in order to delete these data. It is an effective way to delete the data by

adopting convex polygon frame selection method. Application and Implement of the algorithm is simple, including the following two steps. (1) To work out the computer screen coordinate of all points by using the 3D point clouds data; (2) To judge and delete the point data in 2D convex polygon. The detailed process is presented in the figure 3.1. The method of working out screen coordinate is the core of OpenGL technology. See the detailed information in Chapter 5. Next, we will interpret how to judge whether the points are on the convex polygon or not.

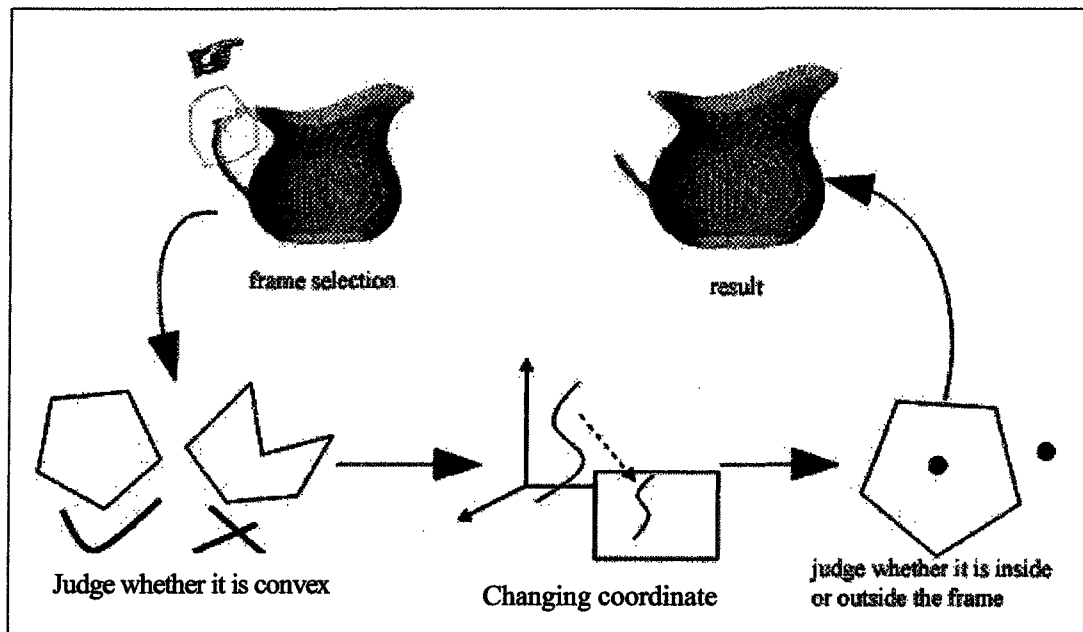


**Figure 3.1** Flow of frame selection to delete point data

The method of judging points within convex polygon is very fundamental and ordinary in computational geometry [34]. There are many algorithms and methods which can be exerted. “The process of them can be divided into two steps: First, judging whether the polygon of frame point cloud data is convex polygon. Then judge whether the point is

within the polygon.” The general algorithms can be implemented directly for convex polygon. But it is not suitable for concave polygon. In that case, it can not be implemented easily except by dividing concave polygon into several convex polygon, but the algorithm is rather complex and difficult. In the experiment, methods of processing convex polygon are provided.

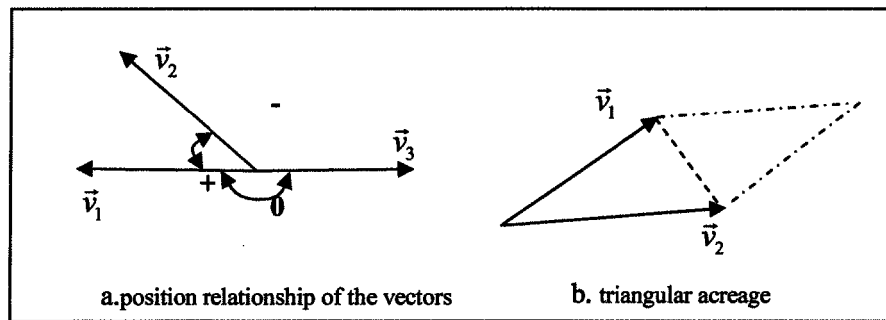


**Figure 3.2** Calculation of 2D vector cross product

The following algorithms are based on 2D vector cross product operation<sup>[59]</sup>. It makes the algorithms of 2D geometry calculation become easier. For the two 2D vector cross product of  $\vec{v}_1(x_1, y_1)$  and  $\vec{v}_2(x_2, y_2)$ , we can express it as following.

$$\vec{v}_1 \times \vec{v}_2 = x_1 y_2 - y_1 x_2 \quad (3.1)$$

The algorithms of 2D vector cross product have two functions: (1) judge the position of two vectors, and see whether it is clockwise or anticlockwise. Combining the expression (3.1) and (3.2), such conclusion can be drawn: if it is deasil from  $v_1$  to  $v_2$ , the result of cross product is negative. Otherwise, the result is positive. When  $v_1$  and  $v_2$  are in the same line, the cross product is 0. (2) calculate the area of the triangular formed by the two vectors as edges, see Figure 3.2(b), it can be expressed as the following.

$$S_{\Delta} = \frac{\|\vec{v}_1 \times \vec{v}_2\|}{2} \quad (3.2)$$

“If we extend any edge of polygon to two directions and the others edges are at the same side of extending line, then this is a convex polygon”<sup>[59]</sup>. We can judge the shape of polygon according to the definition. But implementation of the algorithms is very complicated. The available method is to exert 2D vector cross product in order to judge the shape of polygon. Calculate cross product of two neighboring vectors in turn. If all the result is positive, it is convex polygon. If there contains negative result, then it is concave polygon.

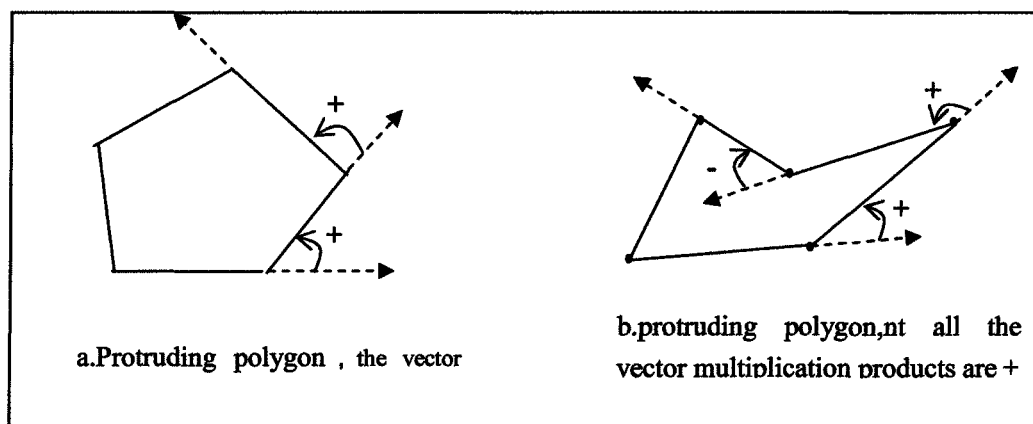


**Figure 3.3** Judge the shape of polygon (from the reference [59])

To judging whether point P is within concave polygon, we can observe to search for it directly. The other two main methods are introduced as follows.

(1) The method of acreage<sup>[60]</sup>

Compare the acreage difference between the triangle which is circulated by the judging point and vertexes of edges and the polygon. Shown as in Figure 3.4, “the acreage of polygon can be obtained by calculating the sum of triangular acreage linked by all

points sequent including inside points, points on the line, and the others points on the line”, just like the figure3.4(b)  $S_1 = S$ . But if the judging point is outside of the polygon, the result is not the same, just like the figure3.4(c)  $S_2 \neq S$ . Therefore the algorithms may help us to judge whether the judging point is within the polygon or not. Because the implement of algorithms belong to the calculation of floating points, errors in judgement may be committed.

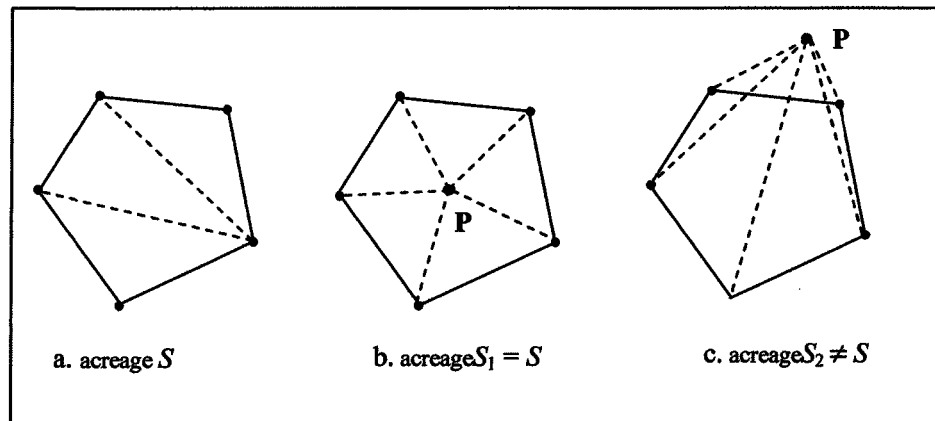


Figure 3.4 The method of acreage

## (2) Method of vector sequence cross product

In the experiment, the algorithms of vector sequence cross product is utilized by the following steps: Suppose  $N$  vertexes in convex polygon are stocked in linearity list vertex  $[N - 1]$ ,  $P$  is a point to judge, shown as in the Figure 3.5(a). For each vertex of polygon and each line, we can confirm the following vectors and cross product <sup>[35]</sup>.

$$\begin{cases} \vec{E} = \text{vertex}[i+1] - \text{vertex}[i] \\ \vec{V} = P - \text{vertex}[i] \\ S = \text{sign}(E \times V) \end{cases} \quad (3.3)$$

$S$  is an expression judgment. Numerical value  $S$  is a sign which value ranges in  $\{-1,0,1\}$ . If  $S$  is unchangeable in all edges, namely the value of them is  $-1$  or  $1$ , then point  $P$  is within the convex polygon. If for some edged, the value of  $S$  is  $0$ , then the point  $P$  is on the edge of the polygon; if for some edged, the value of  $S$  is  $-1$ , and for the other edged, the value of  $S$  is  $1$ , then point  $P$  is outside the polygon. Take an example shown as in figure 3.5(a) to illustrate. When the point  $P$  is inside the polygon, then the symbols of the cross product are consistent, while when the point  $P$  is outside the polygon, then the symbols of the cross product are contrary to each other. By comparison, this method is easy and practical, which can effectively complete the task of deleting the redundant point data. Figure 3.6 is the effect of deleting redundant data by polygon frame-selection algorithm, which displays the point clouds data of scanning a standard sphere, the redundant data points are derived from scanning the platform which is used to fix up the sphere.

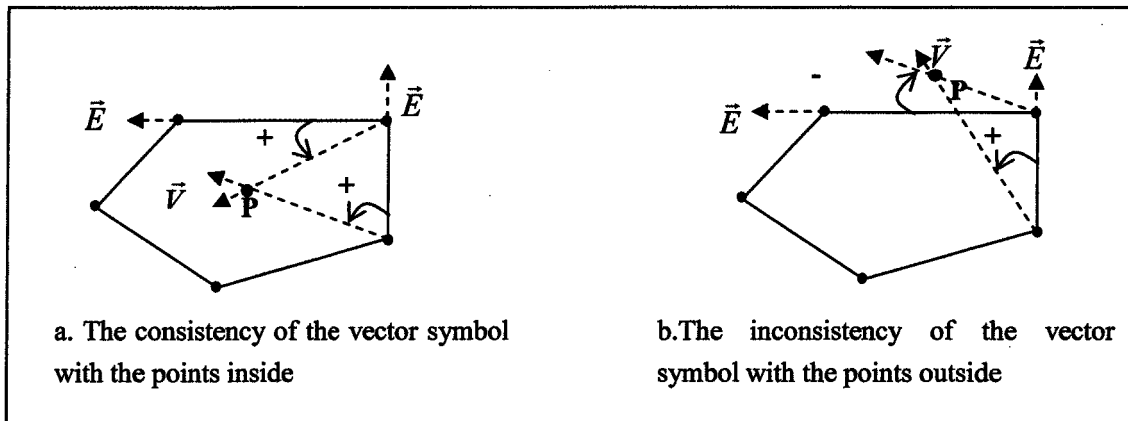


**Figure 3.5** Method of vector sequence cross product

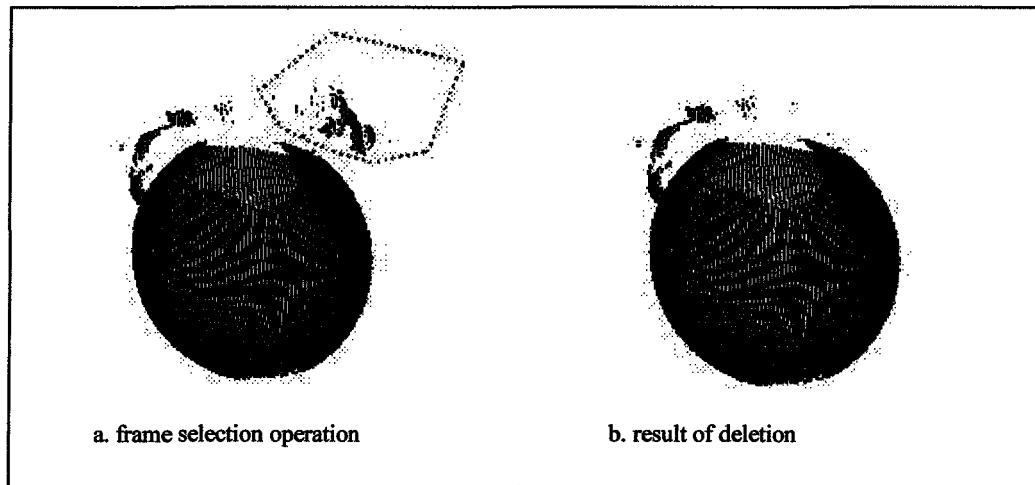


**Figure 3.6** The effect of polygon frame-selection algorithm

### 3.2 Noise Data Deletion

As what is said above, in the scanning process, influenced by the environment and the measuring system, the data points are vulnerable to the disturbing data. So the operations of noise data deletion and smoothing of point clouds data are necessary. Those points with the trait of jumpiness are usually isolated from the point clouds data, so they are called spikes or isolated points. The frame selection method mentioned in the last section can also be used in deleting these points, but the large amount of manual deletion by the users can not guarantee the completeness of the job. So the method of system automatic judgment should be added. In the experiment, the processing method by combining the manual and systematic judgment together is more effective in deleting the noise point data.

### 3.2.1 Noise data deletion by system judgment

For the point clouds data, there are two numerical values which can describe the molding information of the points sequence. (1) See Figure 3.7(a), the angle  $\theta$  between two vectors  $\vec{v}_1$  and  $\vec{v}_2$  reflects roughly the curvature information of  $P_1$ , so it is called curvature angle. The case is that the bigger the angle value is, the bigger of curvature of the current point and the acuter the changing. Otherwise, the curvature is small and the changing is slower<sup>[6]</sup>. For those convex points, the curvature changing is much sharper. General speaking, we can delete these points through the value of vector curvature. As regard the laser scanned free curved surface, the curvature changing is usually not very sharp, or we say there is an upper limit. So in system judging by this value, we need to determine an upper limit for the angle value, the points which are bigger than this upper limit are regarded as convex points and they will be deleted. (2) Shown as in Figure 3.7(b), we link the first scanning point  $P_0$  and the third scanning point  $P_2$  by a linear, then the shortest distance between  $P_1$  and the line  $P_0P_2$  is defined as the height  $h$  of chord  $\square P_0P_1P_2$ , we can work it out by the following formula.

$$h = |P_0P_1| \sin \alpha \quad (3.4)$$

Here,  $\alpha$  is the angle between the two vectors  $\vec{v}_1$  and  $\vec{v}_2$ .  $||$  is the length of the segment. The same to the curvature angle, there is an upper limit for the chord length in the different curved surface. While the chord length of the convex points is bigger than this

upper limit. So we can delete these convex points by determining an upper limit of the chord length in system judgment <sup>[36]</sup>.

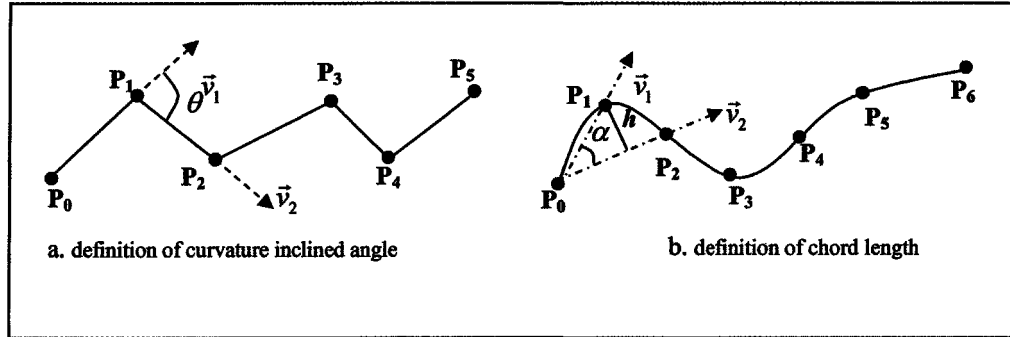


**Figure 3.7** The description of points position information

### 3.2.2 Point clouds data smoothing algorithm

The aim of smoothing algorithm is to average the errors produced while measuring, and obtain the quite smooth point clouds distribution. But there must be some changes on the original scanning point in smoothing algorithm, even some of them possibly can cause some distortion in the reconstructed model. The smooth algorithm mainly has the following several kinds <sup>[37]</sup>: median, mean value and Gaussian.

(1) the principle of median algorithm is to replace the original points with the average value of three points on the scanning line. Supposing the adjacent three points are respectively  $x_0$ ,  $x_1$  and  $x_2$ , then the new point acquired is as follows.

$$x'_1 = (x_0 + x_1 + x_2) / 3 \quad (3.5)$$

And replace the point  $x_1$  with it, shown as in Figure 3.8(a).

(2) mean value algorithm is to replace the original point with the core of the adjacent three points, shown as in 3.8(b). And replace  $x_1$  with the core of the triangle formed by the three adjacent points, namely  $x'_1$  is on the line linking  $x_1$  and the middle of edge  $\overline{x_0x_2}$ , and away from  $x_1$  by  $\frac{2}{3}$  of the midline;

(3) Gaussian algorithm is to delete the high-frequency noise with Gaussian filter and not only realizes smoothing but also avoids the contraction in processing algorithm by revision algorithm proposed by Taubin. The detailed implementation will be further explained in mesh smoothing algorithm of chapter 4.

Figure 3.9 is the effect comparison of one scanning line in sphere point clouds data by median algorithm before and after processing

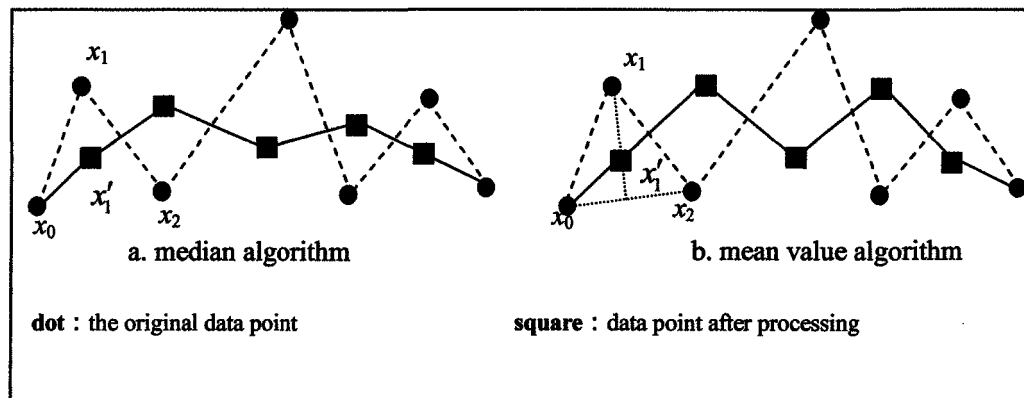


**Figure3.8** Point data smoothing algorithm

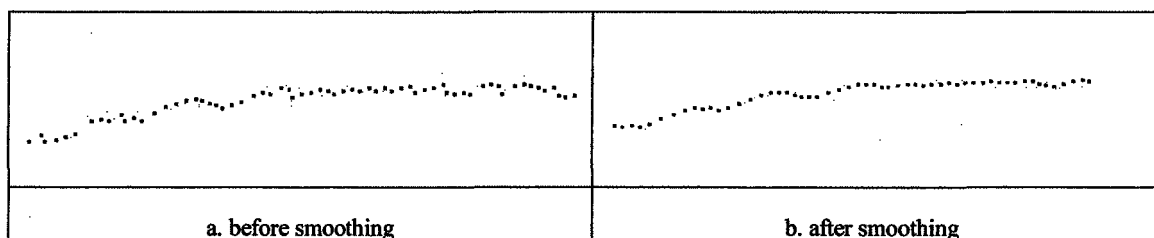


**Figure3.9** Effect of median algorithm processing

### 3.3 Data Simplification Algorithm

Data simplification algorithm implemented the data sampling of the scanning point clouds data in order to reduce the complexity in the following processing algorithm and to enhance the processing speed. The principle of data simplification is to reduce the nonessential data information as far as possible while guaranteeing the real characteristics of the curved surface. The data sampling method approximately may divide into simple sampling and curvature sampling.

The simple sampling is the regular sampling of the point clouds data in quantity and space, which is the most basic sampling method. But although it may reduce the data quantity, it cannot guarantee the very good characteristic of the object curved surface. While the so-called curvature sampling refers to sampling more data in the place where the curvature of the object has many changes; otherwise sampling less data points. This method conforms to the object modeling principle, therefore it may preserve the object curved surface characteristic quite well, which is a frequently used way in point clouds data processing. It mainly includes chord length and grid two method. Now, we will specifically explain the processing courses of each kind of data simplification algorithm.

#### 3.3.1 Factor algorithm

In this algorithm, firstly we must assign an unitary curtailment proportionality factor  $n(n > 3)$ , and sample data in each scanning line with it. That means to reserve the

beginning point and ending point of each line, and then sample data every other  $n-2$  points. This algorithm only carries on the corresponding search of the scanning data, therefore the speed is very quick, and it is quite suitable for those regulate point clouds datas and the objects with slow changing in curvature. It is suitable to the data obtained in different scanning way. But it is only one simple sampling algorithm and cannot guarantee the characteristic of the curved surface is not distorted.

### **3.3.2 Spatial algorithm**

There are certain rules in the distance between point data on the scanning line for some certain laser scanning system controlled by scanning system parameters. Point clouds data sampling based on a spatial distance is principle of spatial algorithm. Firstly a sampling distance value  $d$  must be determined. If the distance between one data point and its preceding data point surpasses this value, then this spot is retained, otherwise it is deleted. According to this method, judging and processing the points on the scanning lines in turn and implement the simplification of data. The same to other simple sampling algorithms, this algorithm is also quite suitable to the curved surface with slow curvature, for the curved surface changing fiercely, the algorithm possibly can reject some key points which are needy in the reconstruction of the curved surface. But the spatial algorithm has considered the distance changing in scanning space so it is superior to factor algorithm.

### 3.3.3 Height decision algorithm

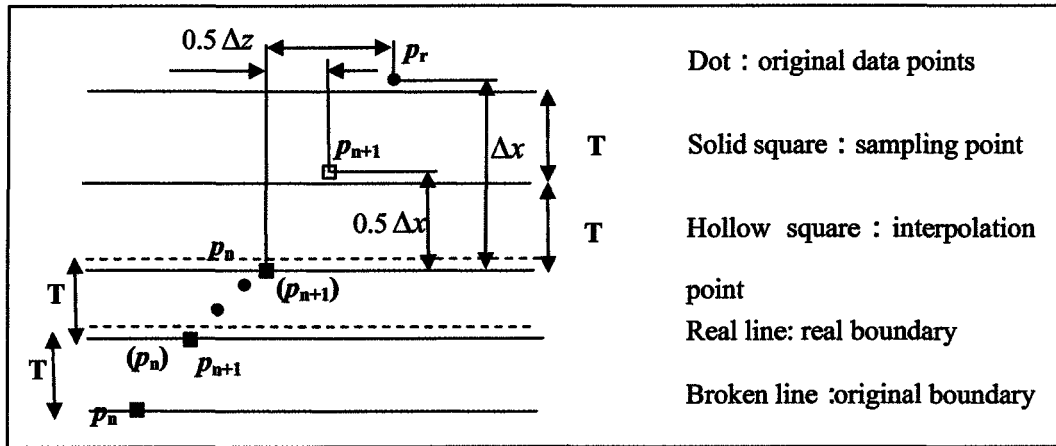


Figure 3.10 Height Decision algorithm diagram

In chapter two, we mentioned that the point data on the chord direction in the translating scanning line changes according to some rules. Height decision algorithm simplifies the point clouds data according to these characteristics. Set up a sampling distance  $T$  in cord direction , then judge in turn from the first point on the scanning line, shown as in Figure 3.10. And set  $p_n(x_n, y_n, z_n)$  as one retained point, and retain another point on its adjacent height  $T$  and hold this point as  $p_{n+1}$  ; If there are many points , then retain the one which is the nearest to  $T$  boundary as  $p_{n+1}$  ; and if there is no data point in the scope of  $T$  , that means there is little change in curvature, and the interpolation points are unnecessary; otherwise, it there are still no data points in the scope of two  $T$ , use the following way to interpolate:

$$\begin{cases} p_{n+1}(x_{n+1}, y_{n+1}, z_{n+1}) = (x_n + 0.5\Delta x, y_n, z_n + 0.5\Delta z) \\ \Delta x = x_r - x_n, \quad \Delta z = z_r - z_n \end{cases} \quad (3.5)$$

Take Point  $p_{n+1}$  as the start point of the next judgment and carry on the same

judgment. In fact, we can see from the following experiment result, this kind of sampling can't avoid the molding distortion either.

### 3.3.4 Chord algorithm

Chord algorithm is a sampling algorithm of point clouds data<sup>[57, 58]</sup>. According to the definition of chord length mentioned in the above part, we can calculate the chord length of the given points circularly, and compare it with the given chord length to simplify data. In this sample process, the algorithm takes the judgment of the molding characteristic value of the object into consideration, thus guarantees the real characteristic of the point data reconstruction. The concrete algorithm is as the following.

Firstly, set a chord length judgment value  $S$ . Calculate the length of chord  $\overline{P_0P_2}$  from the first point  $P_0$  on a scanning line, namely  $h_1$  in the Figure 3.11. If  $h_1 > S$ , then reserve  $P_1$ , and take it as the start of next circular judgment, and calculate the length of chord  $\overline{P_1P_3}$  according to the same method and carry on judgment; But if  $h_1 < S$ , then delete  $P_1$ , and calculate the chord length of  $\overline{P_0P_3}$ , namely  $h_2$  in Figure 3.11, in the meantime calculate the chord length  $h_3$  of  $\overline{P_0P_1P_3}$ , if there is a value bigger than  $S$  then reserve  $P_3$  and take it as the start point of the next round of circular judgment. Such process will proceed until the last point of the scanning line, those points which are not in accordance with the requirement of chord length will be deleted. Among them, the chord length value  $S$  is defined in advance, and it is the key which decides the ratio of data

simplification. It can be easily concluded that the smaller  $S$  is, the bigger the curvature, otherwise the curvature is smaller. So in simplifying data by chordal algorithm, the certain chord judgment value should be selected according to the various point clouds data. Figure 3.12 is a diagram of the procedure of scanning line simplification by chordal algorithm.

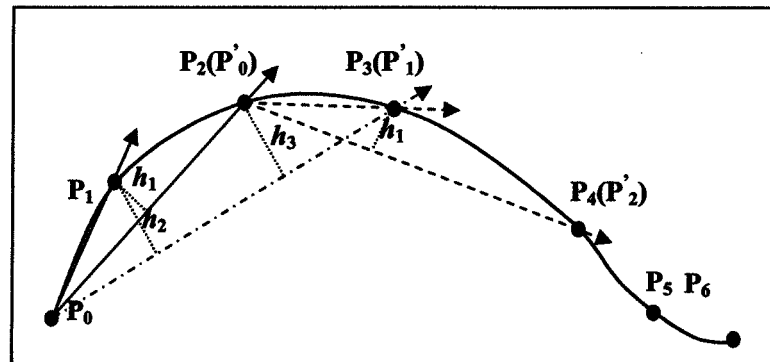


Figure 3.11 Chordal algorithm diagram

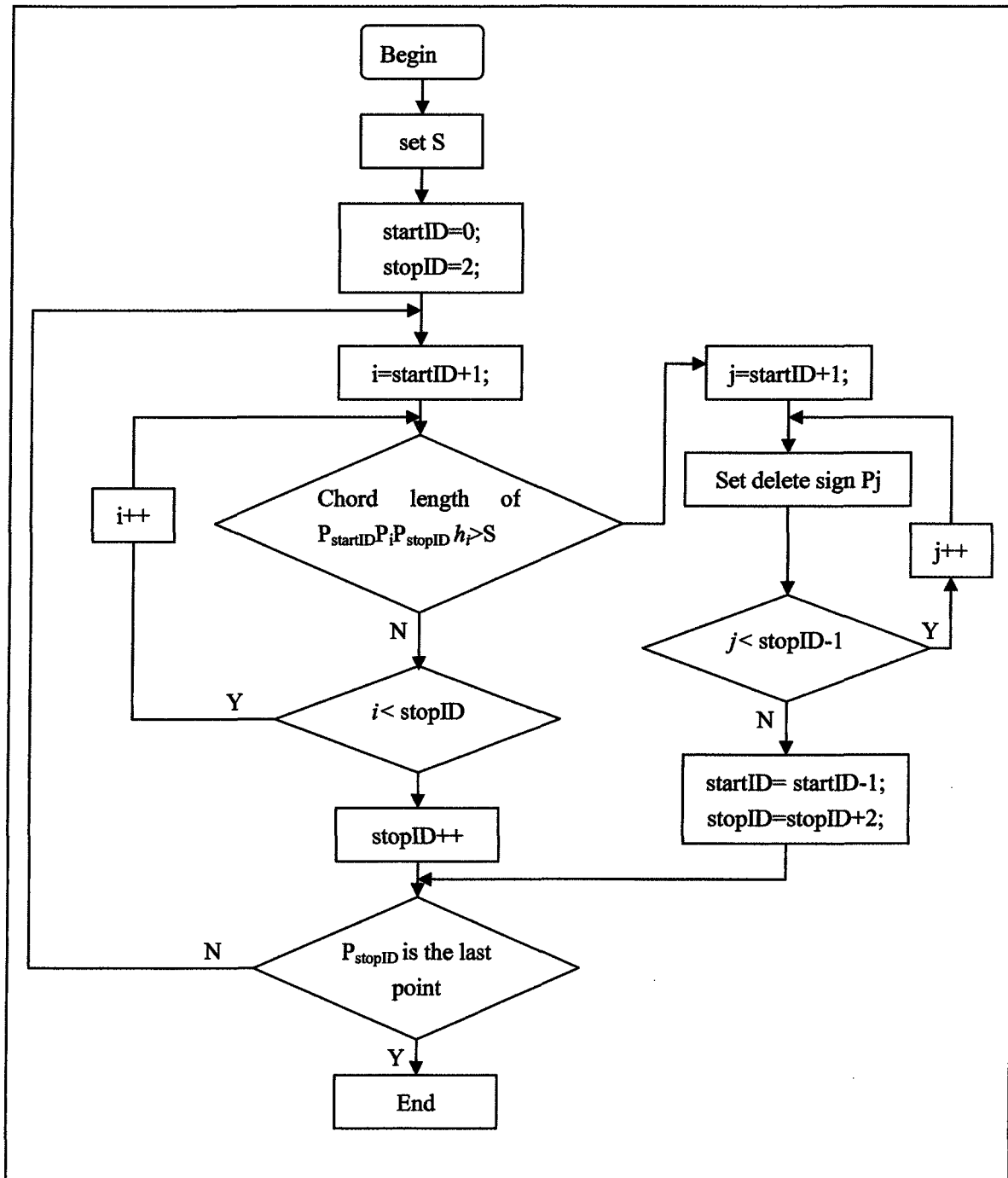
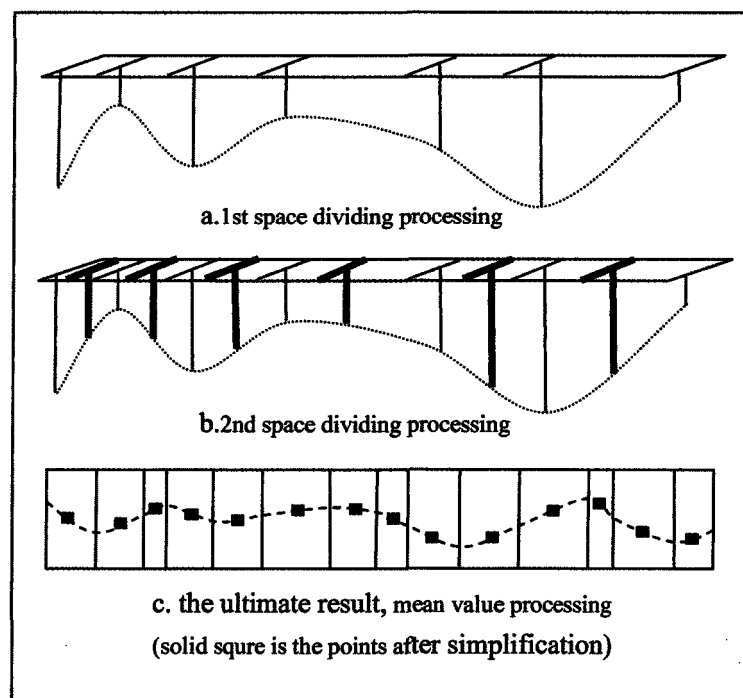


Figure 3.12 Chordal algorithm procedure

### 3.3.5 Grid algorithm

Grid is one kind of data simplification [7] proposed by South Korean researcher K. H. Lee and the others. The same to height decision algorithm, this method is also a standard grid processing algorithm only that the criterion the grid algorithm based on is the size of the curvature included angle and the minute standard size is not fixed. Therefore it surpasses height decision method and it can retain curvature characteristic of the model. The Concrete realization process is shown as the following.



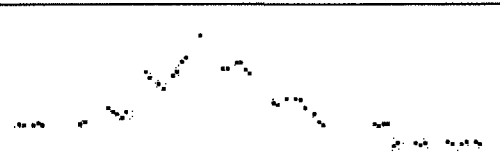
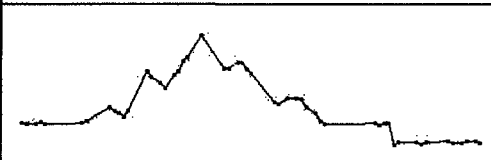
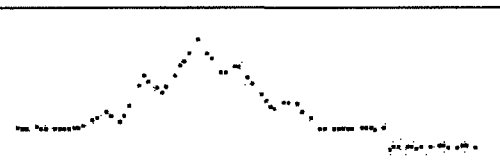
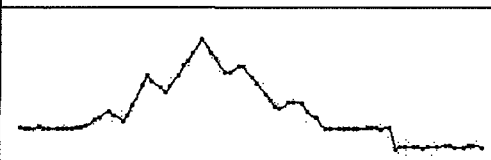
**Figure 3.13** The diagram of grid algorithm processing

Set the minimum value  $T$  of a grid space size firstly, then find out the biggest several points forming biggest several curvature angle and then space dividing the scanning line. Then further process the points in each grid, in this process, ignore those

grids which are no bigger than  $T$ . So the size of the grids after being processed is no bigger than  $T$ . Finally calculate the mean value of all the points in the grid and to replace these points with the mean value and to obtain the result of simplification. Figure 3.13 is the sketch map that describes the processing process of the algorithm. In this algorithm, all of the calculation of the grid space is the same to the height decision algorithm, namely, carrying on the calculation by the value of  $x$  on the scanning line.

Table 3.1 shows the result of the scanning line simplification obtained by different algorithms. The diagram in the table shows the chart of point data and the opposite points linking chart. Through the latter, we can see the influence degree of the algorithm on the shape of curves. See in the chapter 6 for the examples of the processing result of the whole point clouds data.

| algorithm     | Point Data  | Linking Effect   |
|---------------|---|--|
| Original data |  |  |
| Factor        |  |  |
| Spatial       |  |  |

|                 |   |  |
|-----------------|---|--|
| Height Decision |  |  |
| Chord Length    |  |  |
| Grid            |  |  |

**Table 3.1** Effect of the various simplification algorithms

Through the comparison, we can see that, (1) the simple sampling algorithm affects the curve shape, but the curvature sampling algorithm can avoid the shape distortion phenomenon; (2) the usage of chord length algorithm may reduce mass data; (3) besides, the above curvature sampling algorithm has its respective applicable scope. For the rotating scanning data, chord length algorithm can obtain a better effect; but the grid algorithm suits more to the point clouds data gathered by translating scanning way. Actually, after the point cloud data has established the corresponding grid topology, we may carry on the corresponding data simplification called mesh simplification algorithm, it can reduce the data from the overall structure of point clouds data. The detail will be explained in the next chapter.

### **3.4 Adjustment of Simplification Algorithm Under the Restriction of Color Boundary**

If we directly use the above mentioned simplification algorithm in color point clouds data, although some algorithms can guarantee the real characteristics of the object appearance but can't guarantee the color distortion phenomenon. So as long as it is the color data, there will be mutations somewhere in the color information, which is called color boundary. In the reconstruction algorithm which will be mentioned, the color of the reconstructed points is determined through interpolation, which is also the principle of color model demonstrating in OpenGL. If the color boundary is destroyed, the color obtained through the interpolation will be distorted, shown as in figure 3.14.(a) is the primitive color model of the original object. (b) is the color model after the color boundary is destroyed. Therefore, in simplification algorithm, the color boundary restriction must be applied, namely firstly searches the color boundary of the point clouds data, and retain these color boundary points in simplification process. (c) is the color model restricted by color boundary, the color distortion phenomenon has basically vanished.

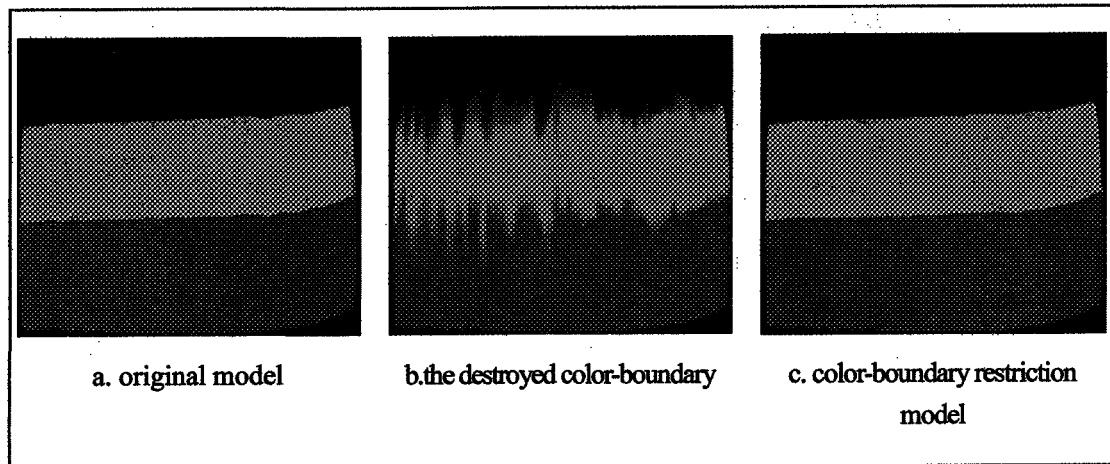


**Figure 3.14** Influences of color boundary on the reconstruction of color model

### 3.4.1 Adjustment of data simplification algorithm under the restriction of color-boundary

Before using the simplification algorithm, we should firstly set the color-boundary.

There are many kinds of color space. The common used ones are RGB and YUV. The general computer display and OpenGL display adopts the RGB color space. It is based on the tricolor principle, and shows the amount of light by tricolor unit. While in RGB color space, any of the color  $F$  can be acquired by the mixing of  $R$ ,  $G$  and  $B$  with proper proportion.

$$F = r \cdot R + g \cdot G + b \cdot B \quad (3.6)$$

Here  $r$ ,  $g$ ,  $b$  is the mixing efficient of color with the scope of the tricolor is between  $[0, 255]$ . RGB color space can be also described as a three-dimensional cube, shown as in figure 3.15. In such space, the difference between colors can be described by the distance

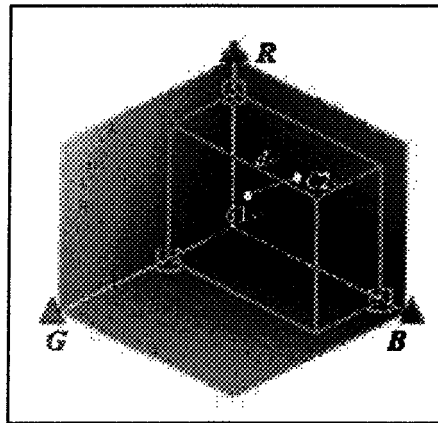
of two points in RGB space, which is called color distance. The bigger the color difference is, the bigger the distance will be. Otherwise it is smaller. Suppose the amount of the color of two points is respectively  $C_1(R_1, G_1, B_1)$  and  $C_2(R_2, G_2, B_2)$ , then the color distance is:

$$d = \sqrt{(R_1 - R_2)^2 + (G_1 - G_2)^2 + (B_1 - B_2)^2} \quad (3.7)$$

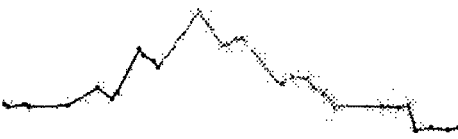
When  $d$  is bigger than some value  $\tau$ , then the two points are regarded as color boundary. And for the convenience of calculation, the following formula can be used to replace the solution formula of color distance.

$$d' = |R_1 - R_2| + |G_1 - G_2| + |B_1 - B_2| \quad (3.8)$$

Search and calculate the scanning line in turn and determine all the adjacent points of the color distance  $d' > \tau$  as color boundary. And here  $\tau$  is a value defined in advance, the result of the experiment show that when  $\tau$  is between 50 and 100, we can get better processing effect.



**Figure 3.15** RGB color space

| algorithm                                  | Color point data  | Connection diagram   |
|--|---|--|
| Original data                              |  |  |
| Simplification data<br>(no restriction)    |  |  |
| Simplification data<br>(color restriction) |  |  |

**Table 3.2** Comparative table of color scanning line simplification

### 3.4.2 The revision of simplification algorithm

After determining the color boundary, then these color boundary restrictions are added to the corresponding point clouds data simplification algorithm. That means the points are on color boundary and retain those which are on the boundary according to the judgment principle of simplification algorithm. But regarding the grid algorithm, the ultimate data is obtained through the solution of mean value. Whereas the color information is not suitable for value processing, we must adjust the grid algorithm of color data simplification by omitting the process of mean value solution and retaining the curvature included biggest angle spot and the color boundary point. Figure 3.16 is the procedure of adjusted grid simplification algorithm of color boundary.

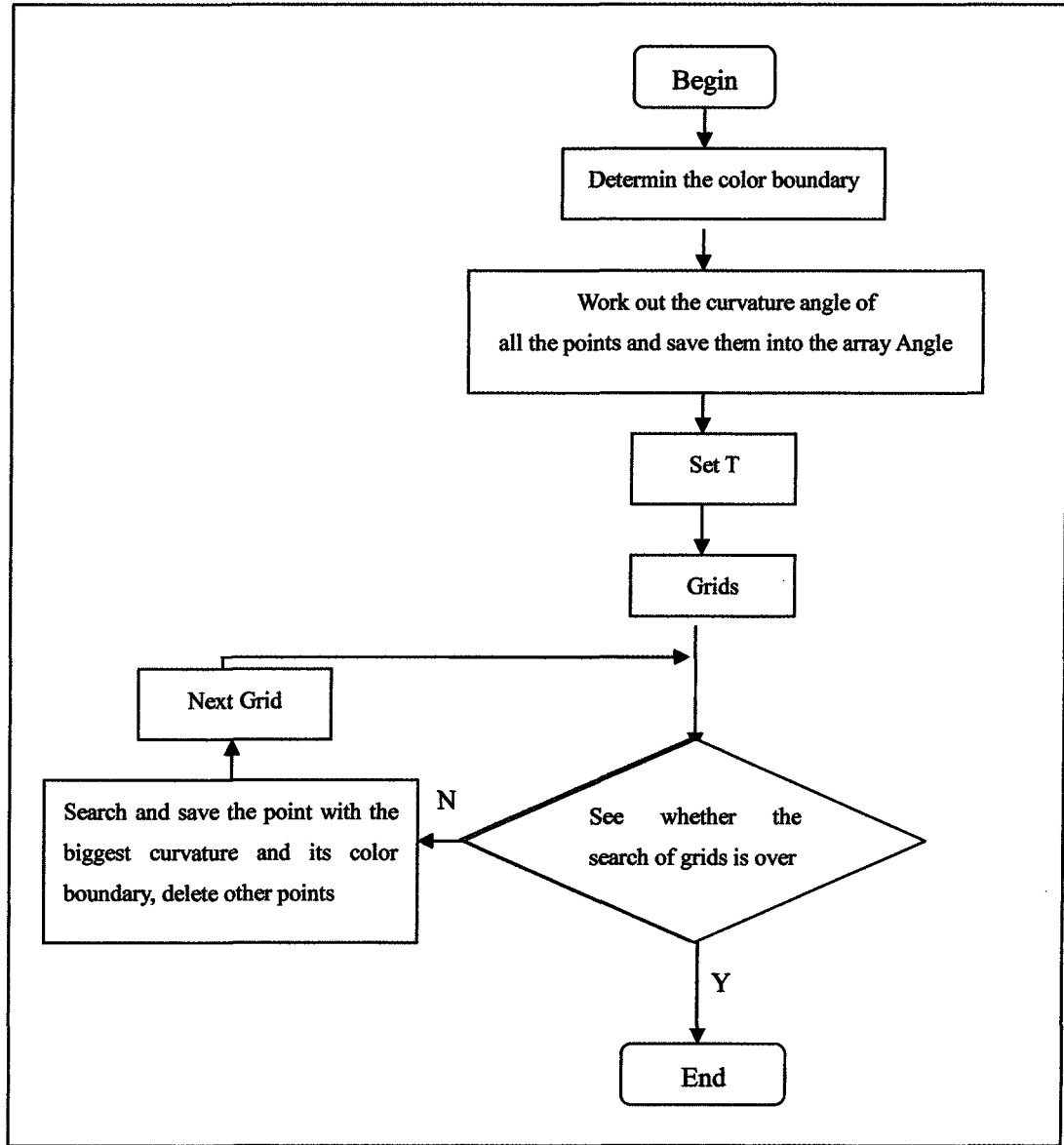


**Figure 3.16** Procedure of grid simplification algorithm of color boundary

The color boundary restraint simplification algorithm not only effectively avoids the model modeling distortion, meanwhile it has avoided the model color distortion, therefore we can obtain the more lifelike color object model through the following reconstruction algorithm processing. Table 3.2 is the effect comparison chart of the color

scanning line processing, the simplification way is the grid algorithm ( $T = 1.8$ ).we may see the point data obtained by color boundary simplification algorithm which keeps the color boundary in good quality. Two examples in the sixth chapter show the effect of the point clouds data simplification algorithm on the reconstructed color model with consideration of color- boundary and non-color-restriction.

### **3.5 Chapter Summary**

In this chapter I described the pre-processing of color laser scanning data, including data simplification, smoothing and noise data deletion. In deleting redundant data, I mainly adopt convex polygon frame selection method and systematic judgment to implement the function. In data simplification many algorithms were mentioned, I mainly designed the function of every algorithm to compare the advantage and disadvantage between the several algorithms according to the different processing results. The post processing, color curved surface reconstruction will be presented in chapter 4 after the pre-processing.

## **CHAPTER 4**

# **COLOR CURVED SURFACE RECONSTRUCTION**

## **CHAPTER 4**

### **COLOR CURVED SURFACE RECONSTRUCTION**

There are two ways of reconstructing point clouds data: Approximation and Interpolation. In Interpolation, it is required that the fitted function and the original points should have the same function value and different coefficient values. But it is still impossible to eliminate the accident errors in measuring. It is difficult to get smoothing model. Because the common B-Spline free curved surface approximation algorithm can realize both the reconstruction of the model and the corresponding smoothing process, mesh reconstruction is needed to reconstruct the color curved surface for the inconvenient one-by-one color addition in OpenGL B-Spline, which is a kind of interpolation algorithm. Mesh reconstruction can describe complex geometry shapes completely and the processing is efficient by using linear operation. Based on the characteristics of free curved surface reconstruction and mesh reconstruction, this thesis sums up the two methods to realize the algorithm and lays emphasis on the smoothing processing using the free curved surface fitting algorithm and the way to reconstruct the color solid model by mesh algorithm. In order to enhance the verisimilitude of the mesh model and the displaying effect of multi-resolution ratio and reduce the capacity of data storage, further smoothing, subdivision

and simplification are required.

#### 4.1 The Fitting of Free Curves And Curved Surface

The common free curves and free curved surfaces in CAD/CAM systems are Bezier , B-Spline and NURBS (Non-Uniform Rational B-Spline Curve). They are one of the most important ways to reconstruct the curved surface and make it smooth. And most of them have good partial control ability, so conveniences for model edition is provided. For approximation algorithm itself, the adoption of Least Mean Square calculating procedure enables it a good way of data smoothing.

##### 4.1.1 Free curve mathematic model

The common mathematic description of curves is expressed by power basis, curve  $C(u)$  is expressed as the following.

$$C(u) = (x(u), y(u), z(u)) = \sum_{i=0}^n \vec{a}_i u^i \quad (0 \leq u \leq 1) \quad (4.1)$$

Here  $\vec{a}_i = (x_i, y_i, z_i)$ . And free curves function realizes the sculpture of various curves by the superposition of subsection functions. The curves on different subsections compound into one part of a complete curve, so each subsection function only influences the local shape of the curve. And the different attributes of the subsection functions make various free curve functions unique. And for each subsection function of Bezier, the control field is indefinite and usually the scope is wide. So the quality of field control is not good

enough and for the subsection function of the other two kinds of free curves, the field scope is certain. So it has good field control ability and is used in wider application.

Another way of describing free curves is by superposing basis functions and control points <sup>[38]</sup>, the expression of B-Spline curve  $C(u)$  is as follows.

$$C(u) = \sum_{i=0}^n N_{i,p}(u) P_i \quad a \leq u \leq b \quad (4.2)$$

Here  $\{P_i\}$  is  $n+1$  control points, each value of variable  $u$  represents only one point on the continuous curve.  $\{N_{i,p}(u)\}$  is a basis function of  $p$  degree B-Spline, expressed by a recursive formula as follows.

$$\begin{cases} N_{i,0}(u) = \begin{cases} 1 & (u_i \leq u < u_{i+1}) \\ 0 & \text{ot her s} \end{cases} \\ N_{i,p}(u) = \frac{u - u_i}{u_{i+p} - u_i} N_{i,p-1}(u) + \frac{u_{i+p+1} - u}{u_{i+p+1} - u_{i+1}} N_{i+1,p-1}(u) \end{cases} \quad (4.3)$$

Here  $\{u_i\}$  makes up a non-degression real number sequence  $U$  and  $a \leq u_i \leq b$ . In general cases,  $a=0$  and  $b=1$ .  $U$  is called knot vector, and the scope of two contiguous elements in the vector is called knot span. From (4.3), we can see that the element number of  $U$  is  $m+1 = n + p + 2$ .

For the given points sequence  $\{Q_k\}$ ,  $k = 0, \dots, m$ , B-Spline curves can be fitted by using the following expression.

$$C(\bar{u}_k) = \sum_{i=0}^n N_{i,p}(\bar{u}_k) P_i \quad (4.4)$$

Here  $\bar{u}_k$  is called Parameter value , corresponding to the given points  $Q_k$  .

The first step is to find out the correct expression of B-Spline curve  $C(u)$  in order to fit the given points sequence with B-Spline. The main tasks to be completed are: Given points parameterization, namely to decide  $\bar{u}_k$ ; To determine the knot vector U; To solve the basis function and control points; To decide the fitting precision for approximation.

(1) There are three ways for parameterization. They are equidistance, chord length and centripetence. And the corresponding formulas are as the following.

$$\text{equidistance : } \begin{cases} \bar{u}_0 = 0, \bar{u}_n = 1 \\ \bar{u}_k = k/n \end{cases} \quad k = 1, \dots, n-1$$

(4.5)

$$\text{chord length : } \begin{cases} \bar{u}_0 = 0, \bar{u}_n = 1 \\ \bar{u}_k = \bar{u}_{k-1} + \frac{\|Q_k - Q_{k-1}\|}{d} \\ d = \sum_{k=1}^n \|Q_k - Q_{k-1}\| \end{cases} \quad k = 1, \dots, n-1$$

(4.6)

$$\text{centripetence. : } \begin{cases} \bar{u}_0 = 0, \bar{u}_n = 1 \\ \bar{u}_k = \bar{u}_{k-1} + \frac{\sqrt{\|Q_k - Q_{k-1}\|}}{d} \\ d = \sum_{k=1}^n \sqrt{\|Q_k - Q_{k-1}\|} \end{cases} \quad k = 1, \dots, n-1$$

(4.7)

In it ,  $\| \cdot \|$  represents the modulus of vector. In equidistance method, the fitted curves are accompanied with some strange phenomena like knots. While the chord length method

is more common-used, by which better parameter value can be acquired; and the centripetence method is more suitable to those data with mutation. And chord length method is also effective in dealing with the relative condensed point data.

(2) There are also three methods to solve knot vector: equidistance, mean value and equal distributing. The formula are respectively the following.

$$\text{equidistance : } \begin{cases} u_0 = \dots = u_p = 0 \\ u_{m-p} = \dots = u_m = 1 \\ u_{j+p} = j/(n-p+1) \quad j=1, \dots, n-p \end{cases}$$

(4.8)

$$\text{mean value : } \begin{cases} u_0 = \dots = u_p = 0 \\ u_{m-p} = \dots = u_m = 1 \\ u_{j+p} = \frac{\sum_{i=j}^{j+p-1} \bar{u}_i}{p} \quad j=1, \dots, n-p \end{cases}$$

(4.9)

$$\text{equal distributing : } \begin{cases} u_0 = \dots = u_p = 0 \\ u_{m-p} = \dots = u_m = 1 \\ u_{j+p} = (1+\alpha)\bar{u}_{i-1} + \alpha\bar{u}_i \quad j=1, \dots, n-p \\ i = [jd] \quad \alpha = jd - i \quad d = (m+1)/(n-p+1) \end{cases}$$

(4.10)

Here,  $[\ ]$  is a sign for selecting whole numbers. Equidistance method is not recommended; mean value method is usually used in interpolation fitting and equal distributing method is usually used to solve  $U$  and it can guarantee that in every knot span of knot vector. There will be one parameter value and such distributing will achieve the

best fitting effect of the curve.

(3) After setting a series of parameters and knot vectors, each basis function  $N_{i,p}(\bar{u}_k)$  can be calculated according to formula (4.3). And the value of each control point  $P_i$  can be calculated by using interpolation and approximation method.

(4) The following equation can be referenced in interpolation fitting algorithm:

$$Q_k = C(\bar{u}_k) = \sum_{i=0}^n N_{i,p}(\bar{u}_k) P_i \quad k = 0, \dots, n \quad (4.11)$$

Namely,  $n+1$  equations determines  $n+1$  control points, and the answer can be easily found by solving the equation group.

(5) LMS (Least Mean Square) algorithm is required in approximation fitting algorithm <sup>[39]</sup>. The approximation fitting curves pass two extreme points instead of the other points. Thus the following expression exists:

$$\begin{cases} C(u) = \sum_{i=0}^n N_{i,p}(u) P_i & u \in [0,1] \\ Q_0 = C(0), \quad Q_m = C(1) \\ f(\bar{u}_k) = \sum_{k=1}^{m-1} |Q_k - C(\bar{u}_k)|^2 = \min \end{cases} \quad (4.12)$$

Under the condition of satisfying the LMS restriction  $\frac{\partial f(\bar{u}_k)}{\partial P_i} = 0$ , the above

expression transforms into the following matrix product.

$$\begin{bmatrix} \sum N_{0,p}^2 & \sum N_{0,p} N_{1,p} & \dots & \sum N_{0,p} N_{n,p} \\ \sum N_{1,p} N_{0,p} & \sum N_{1,p}^2 & \dots & \sum N_{1,p} N_{n,p} \\ \dots & \dots & \dots & \dots \\ \sum N_{n,p} N_{0,p} & \sum N_{n,p} N_{1,p} & \dots & \sum N_{n,p}^2 \end{bmatrix} \cdot \begin{bmatrix} P_0 \\ P_1 \\ \dots \\ P_n \end{bmatrix} = \begin{bmatrix} \sum Q_k N_{0,p} \\ \sum Q_k N_{1,p} \\ \dots \\ \sum Q_k N_{n,p} \end{bmatrix} \quad (4.13)$$

$$\text{Here, } \begin{cases} \sum N_{i,p} N_{j,p} = \sum_{k=1}^{m-1} N_{i,p}(\bar{u}_k) N_{j,p}(\bar{u}_k) \\ \sum Q_k N_{i,p} = \sum_{k=1}^{m-1} Q_k N_{i,p}(\bar{u}_k) \end{cases} \quad (4.14)$$

The matrix expression can be shortened as  $AP=Q$ . We can see that firstly, A is a symmetrical matrix expression, because  $\sum N_{i,p} N_{j,p} = \sum N_{j,p} N_{i,p}$ . And besides, from the B-Spline basis function(4.3), we can get the following.

$$N_{i,p}(u)N_{j,p}(u) \begin{cases} \geq 0 & |i-j| < p \text{ and } u \in U \\ = 0 & \text{Others} \end{cases} \quad (4.15)$$

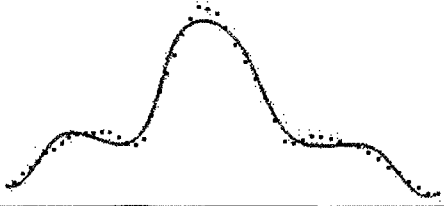
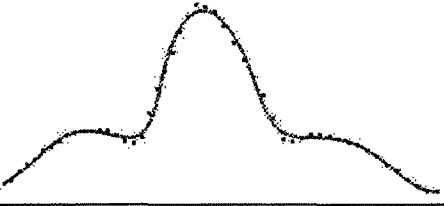
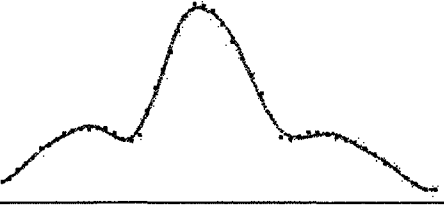
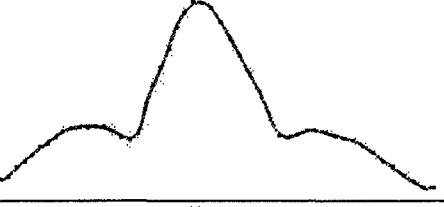
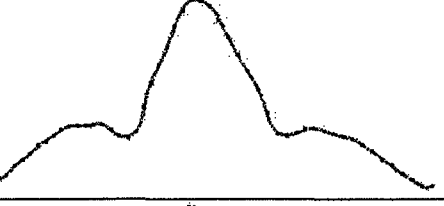
So A is a fixed symmetric matrix array, which can be decomposed into  $A=LDL^T$ . Here, L is a under-triangle matrix, D is a diagonal matrix. And then solve the equation group by chasing method or by Cholesky method, decomposing the fixed symmetrical matrix A into  $A=U^T U$ . Here U is an upper-triangle matrix <sup>[40]</sup>.

(6) For the corresponding relationship between  $\bar{u}_k$  and  $Q_k$ , we can bring  $\bar{u}_k$  into the approximation fitting curves expression (4.2). Then to seek the corresponding point  $Q_k$  in the curves, namely,  $Q_k' = C(\bar{u}_k)$ . Through calculating the mean value of the distance between two points, we can judge the precision  $P$  of the approximation fitting algorithm as the following.

$$P = \frac{1}{m-1} \sum_{k=1}^{m-1} \|Q_k - Q_k'\| \quad (4.16)$$

In the approximation fitting algorithm, the number of the control points  $n$  is changeable. In fact, the fitting precision can be manipulated by changing the number of

control points. Table 4.1 listed the comparison among control points number(*CPN*), the corresponding approximation fitting curve and the fitting precision. Here, the *CPN* is represented by the percentage of the given points.

| <i>CPN</i> (%) | <i>P</i> (mm) | Fitting curve (50points)   |
|----------------|---------------|--|
| 20             | 1.763991      |    |
| 30             | 0.798039      |    |
| 40             | 0.685483      |   |
| 50             | 0.263905      |  |
| 60             | 0.199907      |  |
| 70             | 0.159965      |  |

**Table 4.1** The influence of *CPN* on fitting precision and smoothing degree

From Table 4.1, we can see that (1)The more CPN, the more precise of fitting, and the more closer the fitting curve is to the given points. But the weakness is that it influences the smoothing degree of the curve. (2)Better fitting effect can be achieved when the CNP is from 30 to 60 percent of the number of the given points. (3) When CPN surpasses by 60 percent, there will be some distortion in the fitting curves. For example, there are some distortions in the right extreme of the curve when the CPN accounts for 70 percent in the case of the above table.

Besides, for general curves, the bigger the rank  $P$  of the curve is, the more chances of vibrations will be obtained, and the more complexity of the calculation will be. So in the real fitting process,  $p=3$  is always set up to get  $C^2$  smooth curved<sup>[3]</sup>.

B-Spline is more suitable in dealing with the more plane data points. For those uneven data points, local evenness or spraining phenomena is not a rare case. Comparatively, NURBS is more suitable in dealing with those uneven data points. The curve equation of rank  $P$  NURBS is expressed as the following<sup>[37]</sup>.

$$C(u) = \sum_{i=0}^n R_{i,p}(u)P_i = \frac{\sum_{i=0}^n N_{i,p}(u)\varpi_i P_i}{\sum_{i=0}^n N_{i,p}(u)\varpi_i} \quad (4.17)$$

Here,  $\{\varpi_i\}$  is weights. When  $\varpi_i = a$  ( $a \neq 0$ ) then  $R_{i,p}(u) = N_{i,p}(u)$ . The above expression transforms into B-Spline expression. The introduction of weights influences the manipulation of the control points on curve when it is revised, the curve will move far

away or closer to the given point. So NURBS is commonly used on the editing and molding of curve and curved surface. For example, the skull recovery technique in medicine is an example of taking advantage of the convenience of NURBS molding. While generally, we choose B-Spline to reconstruct the curved surface. Therefore, in the following algorithms, the method of B-Spline approximation fitting curved surface is to be introduced.

#### 4.1.2 Free curved surface reconstruction

In B-Spline curved surface,  $(m+1) \times (n+1)$  control points arrays make up the double network of the control points. Each direction corresponds to a knot vector, that is  $U$  and  $V$  indicated in figure 4.1. B-Spline curved surface equation is as follows.

$$S(u, v) = \sum_{i=0}^n \sum_{j=0}^m N_{i,p}(u) N_{j,q}(v) P_{i,j} \quad (4.18)$$

$$\text{Here, } \begin{cases} U = \{\underbrace{0, \dots, 0}_{p+1}, u_{p+1}, \dots, u_{r-p-1}, \underbrace{1, \dots, 1}_{p+1}\} \\ V = \{\underbrace{0, \dots, 0}_{q+1}, v_{p+1}, \dots, v_{r-p-1}, \underbrace{1, \dots, 1}_{q+1}\} \end{cases} \quad (4.19)$$

$U$  has  $r+1$  knots and satisfies  $r=n+p+1$ .  $V$  has  $s+1$  knots, and satisfies  $s=m+q+1$ .

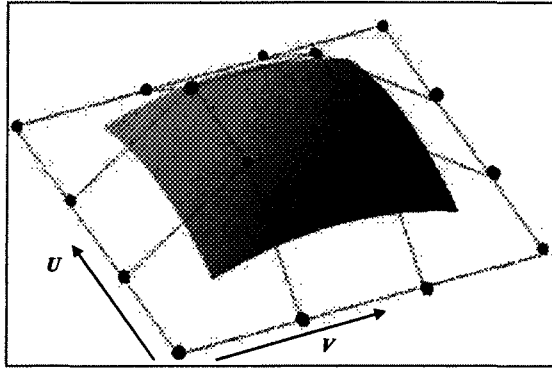


**Figure 4.1** B-Spline curved surface diagram

In order to integrate the given  $(r+1) \times (s+1)$  point clouds data  $\{Q_{k,j}\}$ , two steps algorithm can be used to solve the curved-surface equation.

(1) Transform (4.18) into the following form:

$$S(u, v) = \sum_{i=0}^n \left[ \sum_{j=0}^m N_{j,q}(v) P_{i,j} \right] N_{i,p}(u) \quad (4.20)$$

The above expression can be further separated into two expressions similar to B-Spline curved surface equation just as follows.

$$\begin{cases} Q_{k,i} = \sum_{i=0}^n N_{i,p}(\bar{u}_k) Temp_{i,j} \\ Temp_{k,j} = \sum_{j=0}^m N_{j,q}(\bar{v}_k) P_{i,j} \end{cases} \quad (4.21)$$

(2) Seek the control points each collum of direction U and the above data by the first expression of formular (4.21), namely  $Temp_{i,j}$ . It is a  $(r+1) \times (s+1)$  matrix data in the above expression;

(3) Then to take Temp as the given point data array of the second expression of formular(4.21) to seek the control points on the every line on V-direction and get the

control points of the whole curved surface.

Similar to the integration of the curves, in application, we need to weigh and choose the appropriate number of control points between smoothing and precision degree of the curved surface fitting integration. The criterion is similar to that of curve.

#### 4.1.3 B-Spline curved surface smoothing algorithm

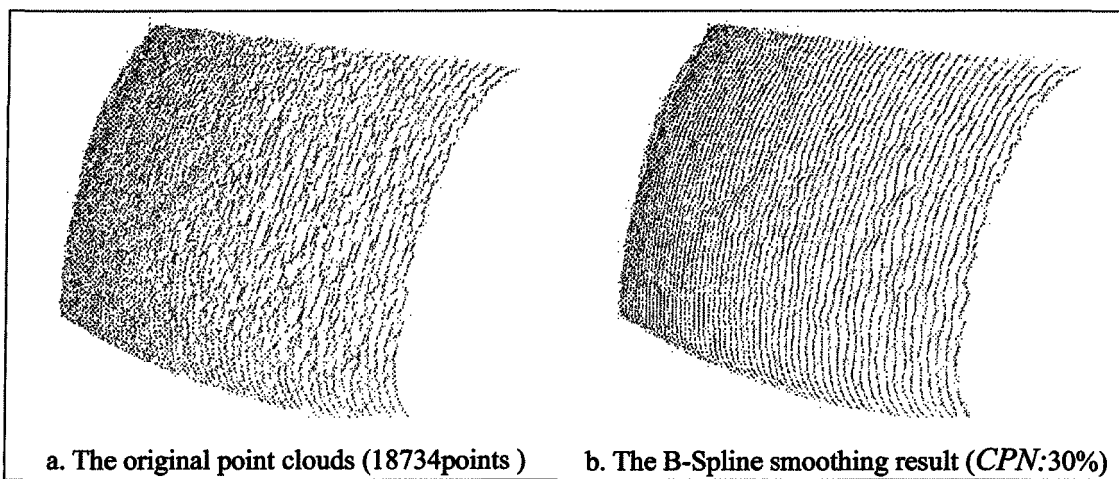


**Figure 4.2** Effect by B-Spline smoothing algorithm

In B-Spline curved surface approximation integration, the usage of LMS can smoothe the data better, so it can also be used in the smoothing processing algorithm of point clouds data. The procedure of the algorithm is as follows. (1) the point clouds data with B-Spline curved surface approximation is integrated to define it mathematically and get expression(4.18); (2)introduce the couple of sequences  $\{\bar{u}_k\}$  and  $\{\bar{v}_k\}$  into formula(4.18), and seek the points on the free curved surface corresponding to the original point clouds data. (3) replace the original point clouds data with the ones which are worked

out reversely, and then the smoothing data can be got by B-Spline surface approximation integrated algorithm. For the controllability of the curved surface integrated control points, we can easily get the point clouds data with different smoothing degree. This algorithm is especially suitable to the processing of those point clouds with poor scanning effect. Figure 4.2 is the processing effect of this algorithm.

## **4.2 Mesh Reconstruction**

In the reconstruction of free curved surface, we can see that the more orderly point clouds data is required. It is matrix array data. So for the general scanning point clouds data, this reconstruction algorithm can not be applied directly. One way is to partitionize the point clouds data or to interpolate or delete the data. Get the orderly point clouds blocks, and then reconstruct the free curved surface. For the partitionized data, the more complex smoothing and boundary restriction process are required in the surface reconstruction algorithm in order to get smooth curved surface[9].

Besides, for OpenGL displaying solid model principle, only the mono-color free curved surface can be realized without resorting to the color chart or the grain operations. In recent years, there are more and more studies on mesh model construction and newly-sprung technology supporting the mesh model such as rapid prototyping, virtual reality, etc. And it is easy to realize the displaying of color solid model for the mesh data especially the triangular mesh data. Mesh constructing model has a loose requirement on

scanning point clouds data and it can completely define the complex solid model, and show the delicate model feature. And the processing generally belongs to linear algorithm. Many software systems have defined the mesh model and have been in good circulation. In the experiment of the subject, the triangular mesh reconstruction is applied in reconstructing the color model.

#### **4.2.1 Scanning data triangular meshing**

According to Lawson's triangle reconstruction principle [13], the triangle meshing should satisfy the following conditions [41] in order to guarantee the best quality in arrangement of the reconstructed triangular mesh surfaces.

(1) The each vertexe of triangle in the triangular mesh is the data points in point clouds and one vertex of which is from one scanning line. The other two vertexes are from the neighboring scanning lines. Namely, each triangle has two spans.

(2) If one triangle passes the line linking two points of the neighboring scanning lines, then there must be another triangular mesh passing this line. Namely each span is the side of two triangles.

(3) Base on the principle of least interior angle the biggest and the shortest side length, the newly-formed triangles can be constructed.

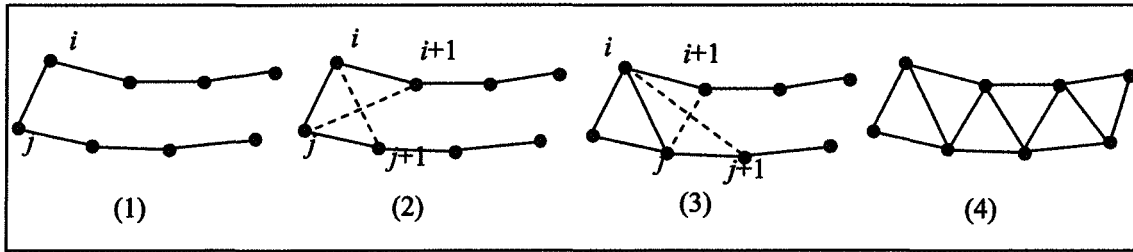


Figure 4.3 Triangular mesh reconstruction rough sketch

For the scanning point clouds data, the scanning lines arrange orderly according to the same direction. So we can use this arrange feature to make the data triangular mesh. Supposing the two neighboring scanning lines separately have  $N_p$  and  $N_q$  points data, and the sequences of  $\{p_i, 1 < i < N_p\}$  and  $\{q_i, 1 < i < N_q\}$  are the points on the scanning lines, then the triangular meshes of the two neighboring lines can be reconstructed according to condition (3). The principle of least interior angle the biggest was proposed by Lawson. In fact, the shortest side length has the same judging principle. And the latter is more easy and practical in application. Figure 4.3 is the rough sketch procedure of constructing the triangle meshes. The procedure is as the following.

- (1) Set  $i = 0$  and  $j = 0$ ;
- (2) Compare the length of  $\overline{p_i q_{j+1}}$  与  $\overline{p_{i+1} q_j}$ . If  $\overline{p_i q_{j+1}}$  is shorter, then construct triangle  $\Delta p_i q_{j+1} q_j$  and set  $j = j + 1$ . If  $\overline{p_{i+1} q_j}$  is shorter, then construct  $\Delta p_{i+1} q_{j+1} q_j$  and set  $i = i + 1$ ;
- (3) If  $j < N_q$  and  $i < N_p$ , then return to step(2). Otherwise jump to step(4);
- (4) If  $j = N_q$  and  $i < N_p$ , then construct  $\Delta p_i p_{i+1} q_j$  and set  $i = i + 1$ . If  $i = N_p$  and

$j < N_q$ , then construct  $\Delta p_i q_{j+1} q_j$  and set  $j = j + 1$ ;

(5) If  $i = N_P$  and  $j = N_q$ , then the algorithm is end. Otherwise it returns to step (4).

After the points on each scanning line in point clouds are constructed into triangular meshes according to the above steps, the mesh model constructing of the whole scanning point clouds data is realized. For the color data, the color information of the interpolation points is acquired from the double-linear interpolation method provided by Gouraud [42]. This process is automatically realized by OpenGL.

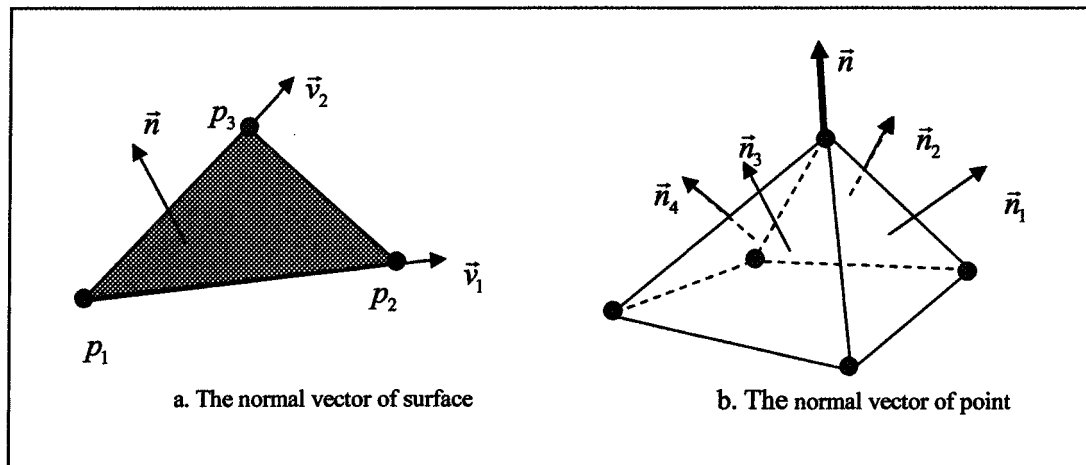


**Figure 4.4** Direction vector calculation rough sketch

In OpenGL, the stereoscopic effect displaying of the model requires the solution of the normal vector. It is solved after the mesh construction. OpenGL provided two ways in adding the normal vectors. One is adding the normal vectors to the surface created by the triangular mesh, the other is adding the normal vectors to each vertex. The latter will show

more delicate model features. The algorithm of the normal vector of triangular meshes is showed in figure 4.4(a). The normalization result of the two vectors ( $\vec{v}_1$  and  $\vec{v}_2$ ) formed by the three vertexes is the value ( $\vec{n}$ ) of the normal vector; while for the calculation of the normal vector of vertexes, the first step is to determine all the triangular surfaces formed by the adjacent vertexes, then the next step is to calculate the normal vector of each surface, finally superimpose and normalize these vectors to get the normal vector of vertexes, shown as in Figure 4.4(b), and the formula is as follows.

$$n = \frac{\sum_{i=1}^m \vec{n}_i}{\left\| \sum_{i=1}^m \vec{n}_i \right\|} \quad (4.22)$$

#### 4.2.2 The Realization Of Triangular Mesh Data Structure

The common data structure can not satisfy the requirement of process efficiency of the mesh. The selected data structure should be convenient to find out the attaching relationship of points, edges and surfaces, which is the elements of forming the triangular meshes. The usually used way is B-rep, which defines not only the solid elements of the triangular mesh but also the inter-relationship between the various elements. There are two kinds of data structures in B-rep: wing-edge structure and half-edge structure [43, 44]. In contrast, topology described by half-edge structure is more sophisticated and the relationship between point, edge and surface can be easily found.

Half-edge structure is a multi-level double list structure. It is made up of five knots:

Solid, Face, Loop, HalfEdge and Vertex. Only three knots are used in the following algorithm: Face represents a triangular mesh; HalfEdge represents one of the half-segments forming Face and arranging clockwise; Vertex is the top point of the mesh, that is the data got after scanning. Figure 4.5 roughly describes their relationship. In half-edge structure, the edges forming the triangular mesh are separated into two parts, called half-edge. This is why the name of data structure comes from. As indicated in Figure 4.5, the two half edges inter-related in structure <sup>[45]</sup>.

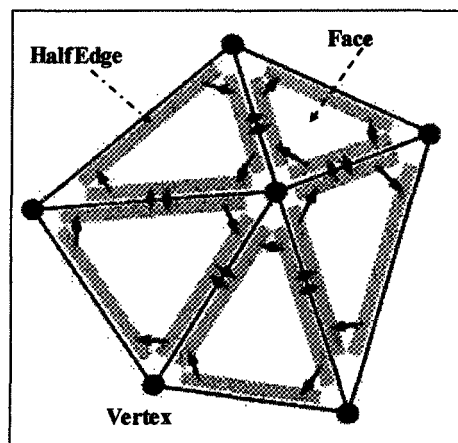


Figure 4.5 Half-edge structural representation

The following is the C++ description of the three knots, which only listed the member variables. Vertex structure includes not only the complete color 3D data of the vertexes ,but also a halfedge list started from the vertexes. The implementation process of C++ is as the following.

```
class Vertex
{
```

```

3DData m_3dinfo;

HalfEdge* edgelist; // all the halfedge lists started from this point

};

```

HalfEdge structure includes halfedge's ending vertex pointer, and that of the corresponding ones facing different direction, also the ones of the connected face containing the halfedge. The realization is shown as the following.

```

class HalfEdge
{
    Vertex* ptrendvert; // the index hand of the half-edge's ending vertex

    HalfEdge * ptrpair; // the corresponding index hand in contrary direction

    Face* ptrface; //the index hand of the face containing this
half-edge

};

```

The variable Face only includes one half-edge list of one composing face. The implementation process of C++ is shown as the following.

```

class Face
{

HalfEdge * edgelist; // the half-edge list composing faces

};

```

In the process of mesh triangularization, all the members of the half-edge initialize according to the topology of triangular mesh. Two important operations need to be finished in order to realize the above-mentioned normal vector algorithm and the following mesh processing algorithm. They are: searching the adjacent point and the adjacent face of one certain vertex. With the help of the above introduced composing parts of data structure and the half-edge list contained in the vertex structure, we can easily find the other vertex linking with this one and the face in which the vertex exists. The employment of half-edge structure is a very convenient way for these two operations.

### 4.3 Mesh Smoothing Algorithm

In the generation process of triangular mesh model, the unavoidable sharp features in the model, resulting from the unsatisfying effect of the previous point clouds data noise deletion, makes the model not enough smooth. So how to further eliminate these noises while maintaining the geometry features of the model has become a hot topic. Some popular mesh smoothing algorithms contains: Laplace algorithm, Taubin's  $\lambda/\mu$  algorithm and Desbrun's average-curvature-based algorithm. These algorithms are different from the direct smoothing process of point clouds data. They are more suitable when the point clouds data are meshed, or when the topology relationship between points is determined. They are an integrated adjustment algorithm of the point clouds data. Laplace smoothing can effectively delete noise but meanwhile it will make the 3D model distort in shape and

contract; Taubin introduced the knowledge of information process into the 3D model processing and proposed  $\lambda|\mu$  method. It is realized the effective low pass filtering through adding a negative contraction element to it and re-enlarged the contraction caused by Laplace smoothing. Desbrun put forward an average-curvature-based algorithm[46], which moves the mesh vertex along normal vector at its average curvature and the effect is proved favorably. In fact, the smooth degree of the model is connected with the mesh numbers composing of model. The more condense of the meshes, the much more smooth the model is. So another way is to add the number of meshes, namely the mesh subdivision algorithm which is to be introduced later. Another aim of subdividing the mesh is to increase the delicate displaying of the model. Even though the local part of the model is enlarged, the details still can be vividly displayed.

#### 4.3.1 Laplace smoothing algorithm

Laplace smoothing algorithm is also called Gaussian smoothing algorithm, in which, each vertex of the mesh is moved to the core of the territory. This algorithm was mentioned in chapter 3. In fact, the principles of the two algorithms are the same, and they are all to determine the domain point of the vertex. Only that for the point clouds scanning line, the domain point only has two adjacent points, while mesh data domain point are determined by the corresponding mesh topology. Such as Figure 4.6, for the  $i$ th vertex  $v_i$  and its first order domain point  $\{v_j\}, j=1, \dots, n$  is like that. That is the

complexity of all the points which share one same edge with  $v_i$ . Laplace's arithmetic operators can be defined as  $\Delta v_i = \sum_{j=1}^n \varpi_{i,j} (v_j - v_i)$ , among which  $\sum_{j=1}^n \varpi_{i,j} = 1$ ,  $\varpi_{i,j}$  is weight which has many ways of selection. The simplest one is to choose the equal weight,  $\varpi_{i,j} = 1/n$ . To choose the reciprocal of the vertex distance as weight, called Fujiwara weight <sup>[47]</sup>, namely  $\varpi_{i,j} = \|v_i - v_j\|^{-1}$ ; And there are also Desbrun and Guskov weights <sup>[47]</sup>. For the later three weights, each process of smoothing requires new solution, so the calculation is complex. With the help of Laplace's arithmetic operators, the vertex coordinate updated into the following.

$$v'_i = v_i + \lambda \Delta v_i \quad (4.23)$$

Here  $0 < \lambda < 1$ , which can control the speed of mesh smoothing. The repetition of the process can eliminate some obvious curvature fluctuations and get better smoothing effect of the mesh data.

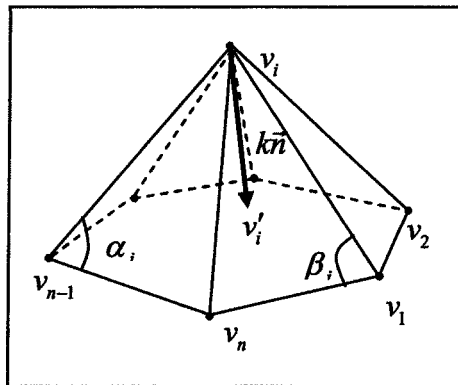


**Figure 4.6** Laplace and Desbrun's smoothing algorithms diagram

### 4.3.2 Taubin smoothing algorithm<sup>[17]</sup>

This algorithm supplied a contrary changing process for each step of Laplace processing, and avoided effectively the contraction phenomena of Laplace. Formular (4.23) is an expression of matrix array.

$$V' = (I - \lambda K)V \quad (4.24)$$

Here  $V$  is a set of the mesh vertexes  $V = \{v_i, 1 \leq i \leq n_v\}$ .  $V'$  is the data after smoothing,  $K$  is a matrix array of  $n_v \times n_v$ , and  $K = I - W$ ,  $W$  is a weight matrix array  $w_{ij} \in W, 1 \leq i, j \leq n_v$ . The expression of Taubin smoothing is as follows.

$$V' = ((I - \mu K)(I - \lambda K))V \quad (4.25)$$

Here  $\mu, \lambda \in R$  and  $0 < \lambda < -\mu$ . If the following expression is regarded as filtering function, just as the following.

$$f(k) = (1 - \mu k)(1 - \lambda k) \quad (4.26)$$

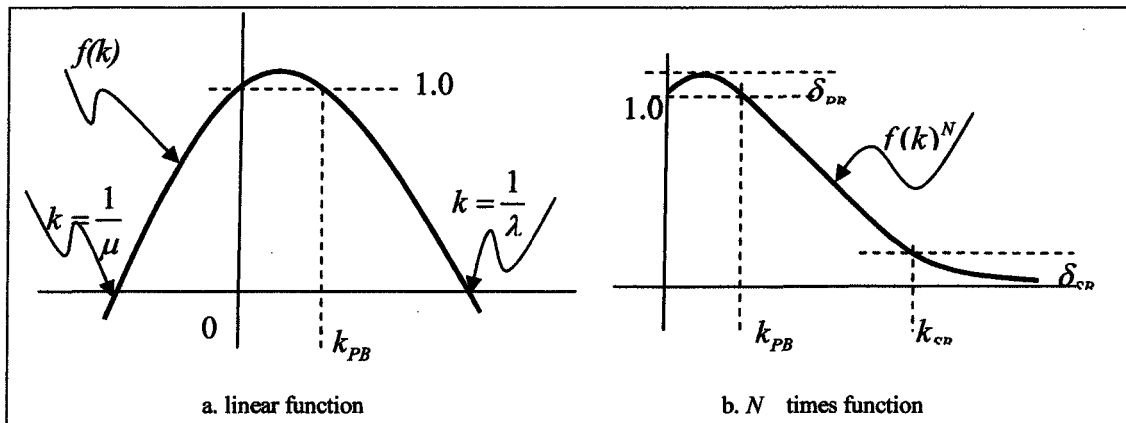


Figure 4.7 Taubin's filtering function

Then the figure of this polynomial is shown as figure 4.7(a).  $k_{PB}$  is defined as the

width of transmission bands and  $k_{PB} = \frac{1}{\lambda} + \frac{1}{\mu}$ . After N times smoothing processes, filtering function  $f(k)^N$  becomes a low pass filtering function with its expression is shown as figure 4.7(b). For the bigger smoothing times N, K is in the transmission bands, that is  $k \in (0, k_{PB})$ ,  $f(k)^N \approx 1$ .  $k_{SB}$  is defined as deadline frequency and  $k$  is in deadline bands, that is  $k \in (k_{SB}, 1/\lambda)$  and  $f(k)^N \approx 0$ .  $\delta_{PB}$  and  $\delta_{SB}$  is respectialy the fluctuation value of the transmission bands and stopping bands.

In the whole algorithm,  $\mu$ ,  $\lambda$  and N are the parameters needed to be put in and their preferred value can be determined by the following expressions.

$$\begin{cases} k_{PB} > 0 \\ \lambda < 1/k_{SB} \\ ((\lambda - \mu)^2 / (-4\mu\lambda))^N < 1 + \delta_{PB} \\ ((1 - \lambda k_{SB})(1 - \mu k_{SB}))^N < \delta_{SB} \end{cases} \quad (4.27)$$

The result of many experiments proved that when  $k_{PB} \in [0.01, 0.1]$ , we can get better smoothing effect. While in determining the value of  $\mu$  and  $\lambda$ , the cycle index N should be within  $k \in (k_{PB}, 2)$  and  $|f(k)| \geq 1$ . The value of  $\lambda$  is better to be larger. Now some common used values of  $\lambda$  mentioned in Taubin's bibliographies are listed, 0.33, 0.314 48 and 0.630 7.

### 4.3.3 Desbrun algorithm <sup>[46]</sup>

Desbrun use curvature flow to guide mesh smoothing. Moving vertex in the direction of normal value at the rate of average curvature. The curvature normal is

expressed with the formula  $\frac{\nabla A}{2A} = k\vec{n}$ , here A is the territory area around vertex  $v_i$ .  $\nabla A$  is the A's derivative of  $v_i$ . And we can get the following expression:

$$-k\vec{n} = \frac{1}{4A} \sum_{j=1}^n (\cot \alpha_j + \cot \beta_j)(v_j - v_i) \quad (4.28)$$

Here  $\alpha_j$  and  $\beta_j$  represents the two angles opposite to the edges  $(v_i, v_j)$ , shown as Figure 4.6. Vertex  $v_i$  is revised by the following expression.

$$v'_i = v_i + \lambda k\vec{n} \quad (4.29)$$

Here  $v_i$  and  $v'_i$  are vectors and we control the speed of mesh smoothing with  $0 < \lambda < 1$ .

Table 4.2 listed the usage and characteristics of the above several smoothing algorithms. Figure 4.8 shows the results of processing of three kinds of smoothing algorithm to a standard ball data. Circulating smoothing 10 times,  $\lambda = 0.5$  and adopt equivalent weights, the consuming time of the algorithms is noted in the brackets (unit:ms). By comparison, Taubin smoothing algorithm is the best choice which takes both processing speed and effect into consideration.

| Smoothing algorithm | Contraction | Processing speed | the determined topology | Data structure | linear\nonlinear |
|---------------------|-------------|------------------|-------------------------|----------------|------------------|
| Laplace             | Yes         | fastest          | Yes                     | Not required   | linear           |
| Taubin              | No          | faster           | Yes                     | Not required   | linear           |
| Desbrun             | No          | Slow             | Yes                     | Not required   | linear           |

Table 4.2 Characteristics Comparison of the common mesh smoothing algorithms.

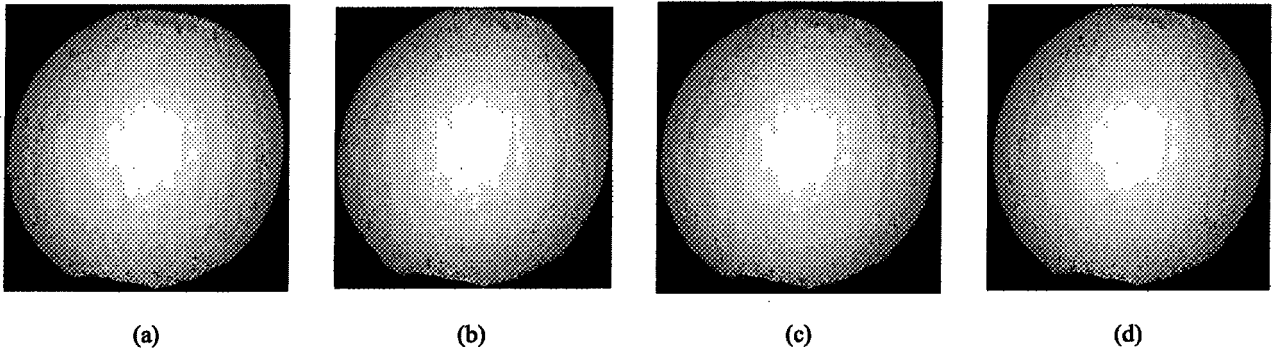


**Figure 4.8** Effect of mesh smoothing algorithms. (a) the original mesh (10122 meshes) (b) Lapace smoothing (47ms) (c) Taubin smoothing (78ms) (d) Desbrun smoothing (3047ms)

#### 4.3.4 Mesh subdivision algorithm <sup>[18]</sup>

There are two kinds of subdivision algorithm commonly used. One is refinement which is suitable for the reconstructed free curved surface. It realizes the subdivision by interpolating and enlarging the control point data, namely adjusting  $\{P_0, P_1, \dots, P_n\}$   $k$  times

into  $\{P_0^k, P_1^k, \dots, P_n^k\}$ . Here  $P_j^k = \sum_{j=0}^n \alpha_{i,j,k} P_j^{k-1}$ ,  $\alpha_{i,j,k}$  is the adjustment coefficient (mask). The

other one is called subdivided, which is a process of the mesh construction algorithm by parting the mesh with newly-added vertexes. The key problem solved by mesh subdivision algorithm to determine the adding position of new vertexes and calculate the coordinate value and color information.

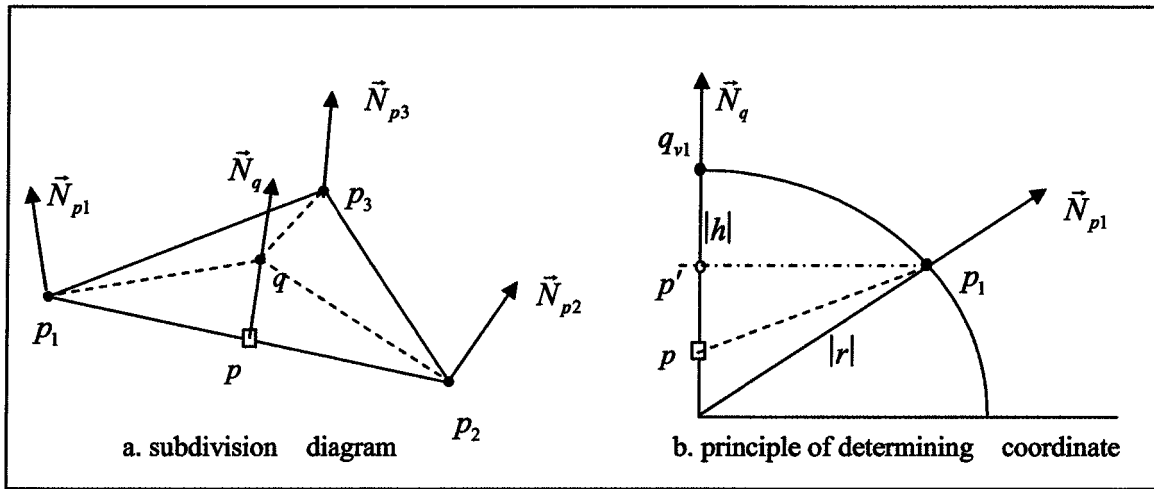


**Figure 4.9** Relationship between new mesh vertices and boundary points

The principle of adding vertices is to judge by the edges of triangle meshes, if the edge is longer than the set shortest length, then add new vertex in the middle of this edge and separate it into two segments. The coordinate of the new vertex can not adopt directly the mean value of the two vertices for the changing curvature of the surface. Volino proposed a Phong vector solution to determine the coordinate value of the new vertices.

For the three vertices  $P_1, P_2, P_3$  of a triangular mesh, the unit normal vectors are respectively  $\overline{N_{p1}}, \overline{N_{p2}}, \overline{N_{p3}}$ , if we want to part the edge  $\overline{P_1P_2}$ , and then add vertex  $q$  shown as in figure 4.9(a). To project  $q$  into the triangular mesh and get  $p$ , the value of  $p$  is  $p = (P_1 + P_2)/2$ , unit normal vector is  $\overline{N_q} = (\overline{N_{p1}} + \overline{N_{p2}}) / \|\overline{N_{p1}} + \overline{N_{p2}}\|$ . The coordinate of the new vertices is the result of taking the three vertices into consideration. Now discuss the new coordinate  $q_{v1}$  influenced by  $P_1$ . Supposing  $q_{v1}$  and  $P_1$  have the same curvature, then there is an arc crossing  $q_{v1}$  and  $P_1$  shown as in Figure 4.9(b) and there are

vectors  $\overline{N}_q$  and  $\overline{N}_{p1}$  which is vertical to it. Then the calculation process is as the following.

(1)  $P'$  is on the linking line of  $P$  and  $q_{v1}$ , and  $\overline{p'p_1} \perp \overline{N}_q$ , then  $p' = p + ((p_1 - p) \cdot \overline{N}_q) \overline{N}_q$ ;

(2) The arc radius of  $q_{v1}$  and  $p_1$  is  $|r| = \|p_1 - p'\| / (p_1 - p') \cdot \overline{N}_{p1}$ , shown as is 4.9(b);

(3) The distance between  $p'$  and  $q_{v1}$  is  $|h| = |r| (1 - \overline{N}_{p1} \cdot \overline{N}_q)$ , shown as in 4.9(b);

(4) The coordinate of  $q_{v1}$  is  $q_{v1} = p' + |h| \overline{N}_q$ .

The new coordinate of  $q$  ( $q_{v2}$  and  $q_{v3}$ ) influenced by  $p_2$  and  $p_3$  can be acquired by the same method, then the ultimate complex coordinate of  $q$  can be got, that is,  $q = (q_{v1} + q_{v2} + q_{v3}) / 3$ . Rearrange the mesh with newly-added vertexes, see Figure 4.9(a), we can see that two new triangular mesh (broken lines part) substituted the original mesh. For the color model, the color information of the newly added points is the mean value of the two vertexes of the partition lines, that is as follows.

$$C_q(r, g, b) = \frac{C_{p_1}(r, g, b) + C_{p_2}(r, g, b)}{2} \quad (4.30)$$

Figure 4.11 is the effect of twice mesh subdivided the point clouds data of the plane scanning flowerpot. The content in the brackets shows the amount of meshes.

#### 4.4 Mesh Simplification

The large amount of triangular faces contained in the mesh model lowered the efficiency of later process and displaying. Besides, in the application in the virtual reality,

the models of different degree of precision are required in order to adapt to the different requirements of displaying effect. Mesh simplification can solve these problems. In recent years, mesh simplification has become the key subject in computer graphics, many methods are proposed, among which Garland's Quadric Error Metrics [48] surpasses the others in time complexity and quality. It can produce high-quantity approximation result while simplifying mesh. For the above reasons, Garland's algorithm is largely used in mesh simplification.

Garland's algorithm belongs to one kind of the circulating edge contraction algorithm, shown as in Figure 4.10. Edge  $\overline{v_1 v_2}$  is contracted into one point  $\bar{v}$ , and  $(v_1, v_2)$  is called a valid vertex pair. While the point  $\bar{v}$  is be acquired through calculating the Quadric Error. The Quadric Error of vertex  $v_1$  is defined as the quadratic sum of the distance from vertex  $v_1$  to all the adjacent planes, that is as the following.

$$\begin{cases} D_1^2 = (\mathbf{n}^T v_1 + d)^2 \\ \mathbf{n}^T v + d = 0 & \text{plane equation} \\ D^2 = \sum_{i=0}^{\text{planesum}} D_i^2 \end{cases} \quad (4.30)$$

Further derivation is got by Quadric Error as follows.

$$D^2 = \mathbf{Q}(v) = v^T \mathbf{A} v + 2\mathbf{b}^T v + c = v^T \mathbf{n} \mathbf{n}^T v + 2d \mathbf{n}^T v + d^2 \quad (4.31)$$

In practical algorithm, we usually substitute Quadric Error by using matrix  $\mathbf{Q}=(\mathbf{A},\mathbf{b},c)$ . So it is called Quadric Error matrix. The following attributes can be proved:

$$\mathbf{Q}_1(v) + \mathbf{Q}_2(v) = (\mathbf{Q}_1 + \mathbf{Q}_2)(v) \quad (4.32)$$

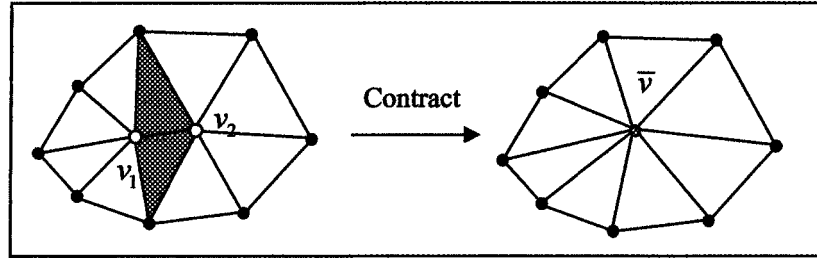


**Figure 4.10** Edge contraction diagram

The norm of judging the  $\bar{v}$  to substitute  $\overline{v_1 v_2}$  is  $\mathbf{Q}(\bar{v}) = \mathbf{Q}_1(\bar{v}) + \mathbf{Q}_2(\bar{v})$ . Here  $\mathbf{Q}_1$  and  $\mathbf{Q}_2$  is respectively the Quadric Error matrix of  $v_1$  and  $v_2$ ,  $\mathbf{Q}$  is the Quadric Error matrix of edge-folded. The detailed algorithm is described as follows.

- (1) To calculate the Quadric Error Matrix  $\mathbf{Q}_i$  of all the vertexes;
- (2) By using  $\|v_1 - v_2\| < t$ ; that means the edge is shorter than the regulate clique value to choose the valid vertex pair  $(v_1, v_2)$ ;
- (3) To calculate  $\mathbf{Q}_1(\bar{v}) + \mathbf{Q}_2(\bar{v})$  of each substitution point  $\bar{v}$  of each valid vertex pair and take it as Quadric Error of  $(v_1, v_2)$ . The value of  $\bar{v}$  can be either  $v_1, v_2$  or  $(v_1 + v_2)/2$ , which is decided on the smallest Quadric Error. The color of  $\bar{v}$  information determines the mean value of two vertexes;
- (4) To put all the acquired valid vertex pairs  $(v_1, v_2)$  and Quadric Error into the stack according to the order of their value, put the smallest on the top stack.
- (5) To output the vertex pairs from the stack by folding and substituting them and adjusting the mesh, shown as in Figure 4.10. And to recalculate the updated vertex pair of

the Quadric Error. Adjust the stack and repeating this process until the stack is empty.

Figure 4.12 is the effect of mesh simplifying of the flowerpot point clouds data. And the content in the bracket is the number of meshes. Figure 4.13 is the effect representation of solid flowerpot and color solid model. We can see that the solid model after mesh simplification is not as clear as the original and the subdivided ones.

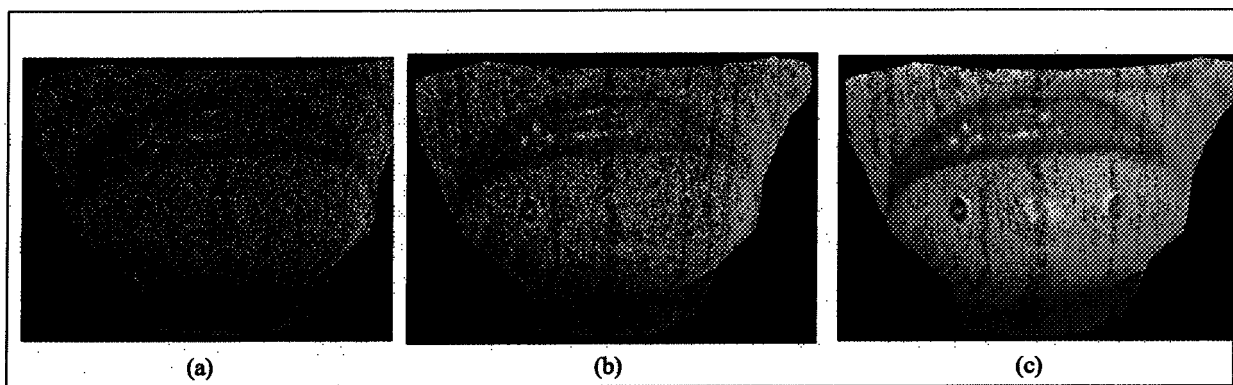


**Figure 4.11** Mesh subdivision effect (a) original mesh (13453) (b) first subdivision (53812) (c) second subdivision (215248)

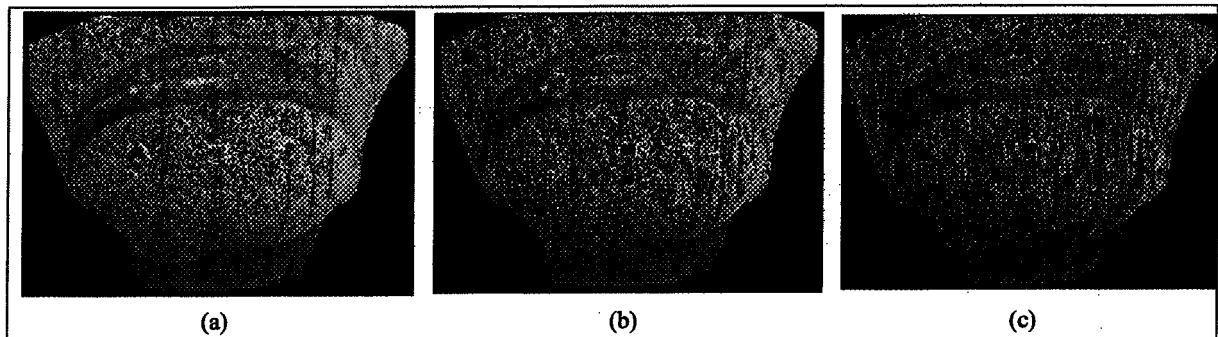


**Figure 4.12** Mesh reduction effect (a) original mesh (20370) (b) first reduction50%(10100) (c) second reduction50%(5007)

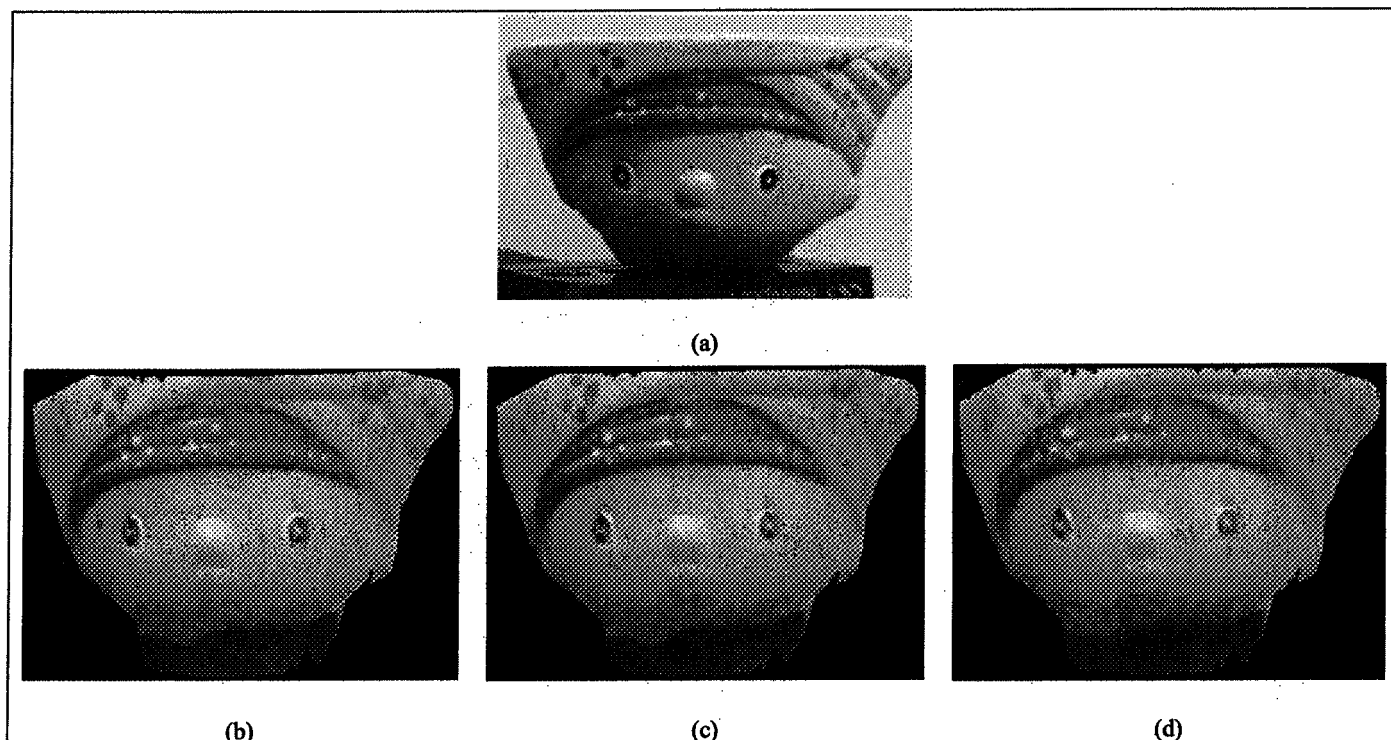


**Figure 4.13** The processing effect of flowerpot solid (a) real image of solid flowerpot (b) original model (20370) (c) subdivision effect (325920) (d) subdivision effect (10100)

## 4.5 Chapter Summary

In this chapter two methods of curved surface and mesh reconstruction was presented to realize the reconstruction algorithm. And I put emphasis on the smoothing processing using the free curved surface fitting algorithm and the way to reconstruct the color solid model by mesh algorithm. It is one of the most important parts in the whole thesis. In the realization of the software, both three-dimensional displaying technology and application interface which will be described in chapter 5 is an essential component.

**CHAPTER 5**  
**3D DISPLAYING TECHNOLOGY AND APPLICATION**  
**INTERFACE**

## **CHAPTER 5**

### **3D DISPLAYING TECHNOLOGY AND APPLICATION INTERFACE**

OpenGL is both a pack of open 3D graphics software and a software interface of graphics hardware. OpenGL pays attention to rapid protracting 2D and 3D models. It is an unarguable standard in current graphics processing engineering and can be used in CAD, emulation, scientific application visibility and game visual fields of true ness. In the processing of color laser scanning data, the optimizing displaying of OpenGL is resorted to. Although OpenGL simplified the difficulty of 3D programming greatly, there is still some unwieldy technology to be dealt with. The following contents will give some technological narration for some common problems in display. Besides, the common used data format of application interface, the realization software processing result, the common 3D software (AutoCAD) and its data exchanging in industrial application (CNC) are analyzed.

#### **5.1 A Brief Introduction of OpenGL Function**

OpenGL is the API library of 3D graphics software development, which contains core library, practical library and assistant library, etc. It is independent from windows

system and operating system. It can replant among the various platforms and has the characteristics of opening, independence and compatibility. The following functions enable OpenGL to be conveniently applied in special graphics processing fields [49]:

(1) It has abundant modeling functions: OpenGL provides not only protracting methods of various simple graphs, but more importantly the protract functions for complex models. For example functions for NURBS curves or surfaces, which makes the 3D model construction more convenient.

(2) It has self-contained coordinate system. It provides coordinate systems, such as world coordinate, view point coordinate, coordinate system etc. The transforming functions between the coordinates, which improves the ability of interaction between man and computers with the functions of conveniently setup and change the position attributes of models.

(3) The setting attributes of illumination, materials and veins not only enable to reappear the real characteristics of the object but also enable to show it more delicately.

(4) Double buffer (foreground buffer and background buffer ) cartoons. In brief, background buffer calculates scenes and forms the menus, foreground buffer displays the finished menus of the background buffer.

## **5.2 The Realization of Key Operations In Displaying**

OpenGL provides convenient and efficient displaying and controlling functions and

reduced largely the difficulty of programming. But in order to display the model correctly, the following set should be paid attention to.

### 5.2.1 Field range adjustment

To display model in OpenGL usually experiences the following transformations, shown as in figure 5.1. in fact, the courses of this processing procedure is completed by multiplication of a series of coordinates transformation matrixes. OpenGL provides for the programmer convenient coordinate transformation functions and saves the complicated matrix multiplication calculation.

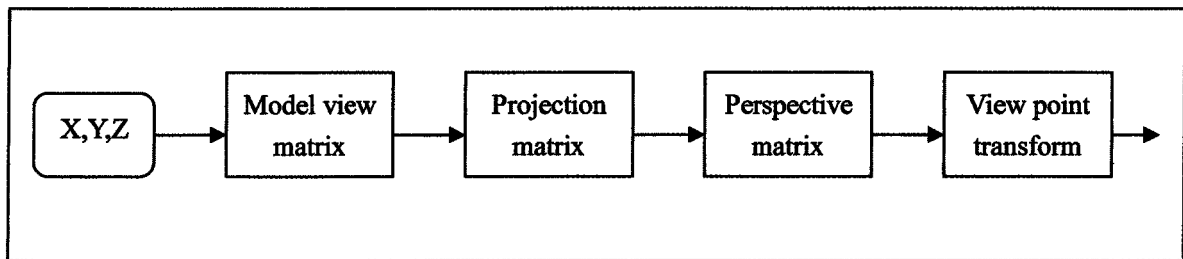


**Figure 5.1** OpenGL displaying processing procedures

OpenGL provides perfect coordinate systems. To display model in the middle of the computer screen and guarantee the feasible human-computer controlling function of the program, the relationship between the various kinds of coordinate systems, especially, the relationship between view point coordinates ( $O_e, X_e, Y_e, Z_e$ ) and world coordinates ( $O_w, X_w, Y_w, Z_w$ ) should be adjusted and pay special attention to. View point coordinate is parameterized by the eyes when we see objects. In acquiescence, view point is in coincidence array with world coordinate origin, shown as in Figure 5.2(a). But view

point coordinate system is left-hand system and the world coordinate system is right-hand system. To display model correctly, the two coordinate systems must be separated appropriately, see figure 5.2(b). OpenGL provided such functions for the coordinate systems as `glTranslate` and `glRotate`, but the usage of this mechanism is not as practical as `gluLookAt` function provided in practical library. It has 9 parameters, ordinarily the world coordinate value  $O_e$  of view point origin, model core coordinate  $O_w$  and the direction vector  $V$  of the view point. Direction vector is defined as the direction of axis  $y$  of the view point system. So the key is to determine the core coordinate of model and the core coordinate of the view point.

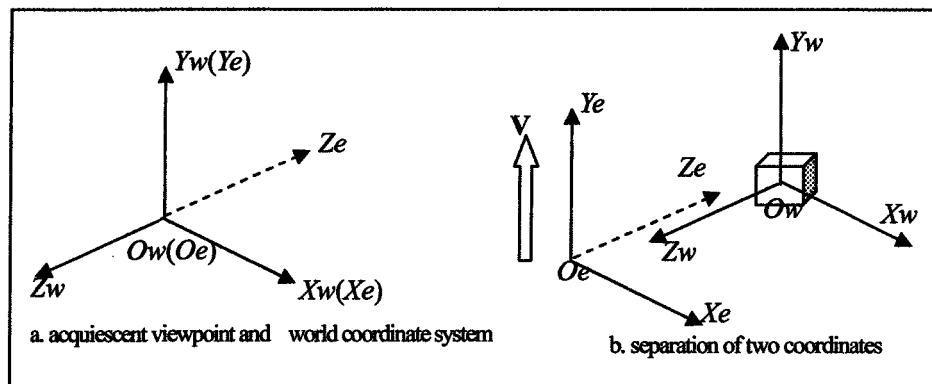


**Figure 5.2** World coordinates and view point coordinates

3D point clouds data can determine firstly the coordinate scope of the displayed object, namely the smallest Boundingbox encircling the object. Then to calculate the coordinate value of the center of Boundingbox, or of the center of sphere outside Boundingbox as the core coordinate  $O_w$  of the model. And in order to determine the

view point core coordinate  $O_e$ , its positional relationship with center coordinate of the model should be firstly determined. Then projection transformation in the displaying procedure should be known about. The aim of projection transformation is to define a viewer and delete the redundant parts, and the ultimate graphics is only the related parts of the viewer, consisting of orthograph and perspective projection, Figure 5.3 is the sketch map of perspective projection, which accords with the people's habits of observation, namely the object is bigger if it is nearer to the view point, otherwise it is smaller until it is dissolved in the farthest way. The viewer in figure 5.3 is the cone parts between the near plane  $Z_{near}$  and the far plane  $Z_{far}$ . `gluPerspective` function set contains four parameters, successively viewing angle  $\theta$ , the projection transformation ratio of width and height and the z coordinate value of  $Z_{near}$  and  $Z_{far}$  (note that  $Z_{near}$  and  $Z_{far}$  are the coordinate value of view point coordinate system). When the viewer is in complete display in the model, the distance  $d$  between view point and viewing angle value has the following relationship:

$$d = \frac{h}{2} \cdot \text{ctg} \frac{\theta}{2} \quad (5.1)$$

Here parameter  $h$  is the height of model Boundingbox. In order to display more scene, the viewing angle should be appropriately increased. While in normal usage, viewing angle  $\theta$  is always be determined in the first place (generally between  $40^\circ$  and  $60^\circ$ ), and then solve distance  $d$  by formula and locate the core coordinate  $O_e$  of the view point. Figure 5.4 is the displaying effect of the adjusted field range, in which the scanned

model is displayed right in the center of the program window.

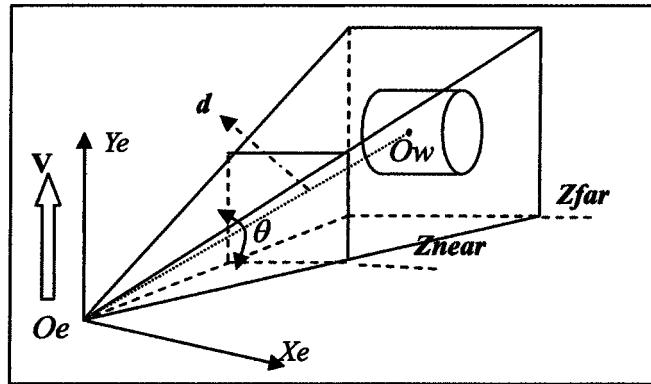


Figure 5.3 Perspective projection sketch map

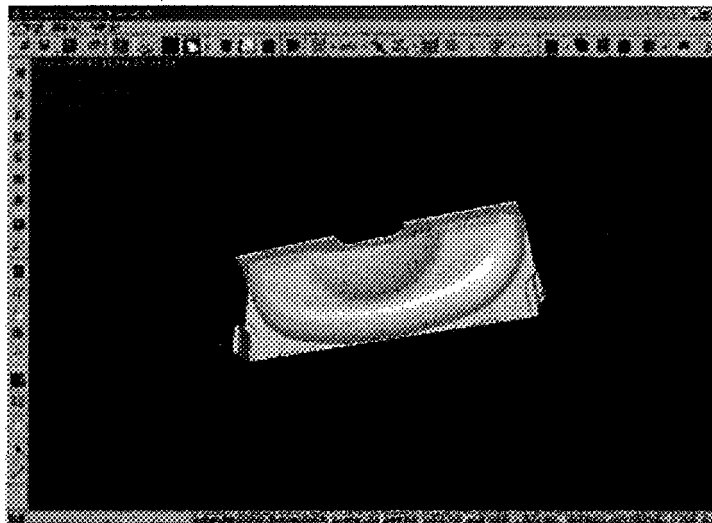


Figure 5.4 Effect of field range adjustment

### 5.2.2 Mouse control

To conveniently control the model and represent the models from different angles, the mouse events should be correspondingly increased to translate or rotate of the model . The fulfillment of the aims of the general mouse control technology is by the way of setting up different references of `glTranslate` and `glRotate` through mouse events, but this

adjustment is not always satisfactory especially in the process of rotating. Because the mouse events in program goes along in 2D space, but the model to be controlled is rotating in 3D space. So in the realization courses of the software, the Virtual Sphere technology proposed by Michael Chen and the others are used, which is a relatively suitable technology in 3D processing, and which realizes the rotating control on models in 3D space by 2D controller. Its principle is: Supposing the model in the screen is encircled by a ellipse ball, and the position of the mouse on the screen is transformed into a point coordinate on the ellipse ball. When the mouse is moving, the movement changing is also transformed into movement on the ellipse ball. Then the rotating coordinate axis and the rotating changing quantity are calculated to acquire the real rotating quantity of the model in 3D space. See the details in bibliography [50].

### 5.2.3 Mutual transformation of world coordinate and screen coordinate

In OpenGL ,the mutual transformation of world coordinate and screen coordinate is a common operation. We can snap the world coordinate correspond to the position of mouse by the movements of the mouse to get the world coordinate by screen coordinate. It can reflect the 3D information of the model. In chapter 3, we mentioned that in the process of deleting redundant data by convex polygon selection, the screen coordinate in the current field of 3D should be acquired. The two steps respectively represent the functions in OpenGL, `gluUnProject` and `gluProject`.

Before using these two core functions, we should firstly get information of the three matrixes in the current field, they are Model view matrix, Projection matrix and Viewport vector. The latter two matrixes are not changing with the rotation and translating movements of the model in the field, so they can be acquired directly before using the core functions. While Model view matrix changes instantly, so it should be acquired after protracting the model field and stored. This can guarantee the accordance of the exchanging matrixes and the model movements. The functions to acquire matrix information are `glGetDoublev` and `glGetIntegerv`. The viewport vector can be got by the latter function and then an integer four dimensional vector is got. The other two are both  $4 \times 4$  floating point matrixs, which can be got by using the previous function.

The procedure to acquire screen coordinate by world coordinate is relatively easy. With the above acquired matrix information, 2D screen coordinate corresponding to 3D coordinate can be acquired directly by `gluProject`. While the procedure to get world coordinate through screen coordinate is not so simple, the depth information of the current screen coordinate is need to be required, namely the third dimension information of 2D screen coordinate endowed by OpenGL. This depth information is stored into a depth buffer memory area, so when we set OpenGL environment, the double buffer memory mode and the depth detection function [51] should be opened. Under this setting, `glReadBuffer` and `glReadPixels` can be adopted to acquire depth information. But without

protracting the area of field, OpenGL can not note down their depth information. So world coordinate of each point in the field can not be acquired correctly and the real world coordinate can not be attained.

#### 5.2.4 Three-dimension quality and sense of reality displaying

The complex model directly protracted in OpenGL is lacking in three-dimension quality. The main reasons are due to the lack of illumination and the normal vector of the vertex. Presented in Figure 5.5. In the real world, without illumination, most objects seem to be not dimensional. The incident light and light absorption and projection of the object determines the scenery people see. And the different object surface can absorb and project different amount of light. It is decided by normal vector on certain place of the objects, which endows the objects with more abundant and exquisite dimensional quality. While the normal vector in OpenGL is divided into two kinds, surface normal vector and point normal vector [52]. For those simple structured graphics, surface normal vector can satisfy the practical requirements without adding vectors for each point with high displaying speed. While for those complex structured models, point normal vector is usually used, because surface normal vector can not satisfy the requirement of reflecting a smooth surface.

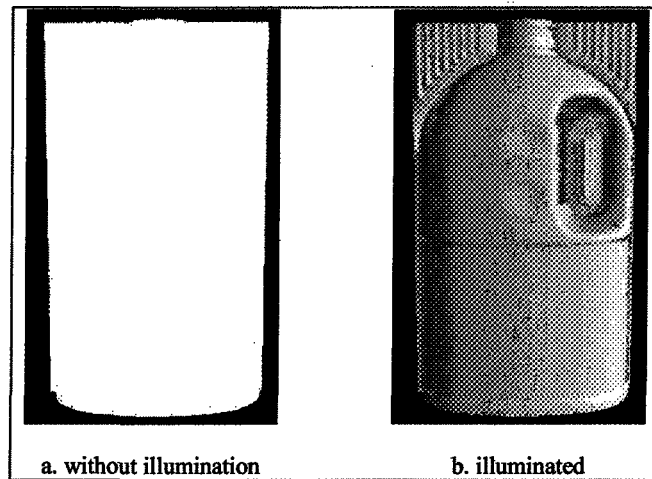


**Figure 5.5** Influences of illumination on field displaying

The illumination models of OpenGL superposed by 4 parts: emitted, ambient, diffuse, and specula light. OpenGL provides 8 light sources for the development staff. Besides the above four attributes, each can be set with the position of light sources and the direction of illumination. The users can achieve their expectant displaying effect by controlling those attributes of the light sources. The adopted function is `glLight`.

OpenGL defines the color of the objects approximately by the projection ratio of the objects' primary colors: red, green and blue. And like light sources, the colors of the objects' material are divided into environmental, diffuse reflection and mirror reflection components. When we calculate the illumination, the components of the material are added into the corresponding parts and superpose with them to display the real color information of the objects and make the displaying in OpenGL authentic. Those objects without setting up the attributes of the material have the three-dimensional quality, but it only reflects the influences of the illumination on the object. The real color of the objects can not be

reflected. There are still something need to be pointed out, that is, in order to display the real color of the objects, white color is strongly recommended instead of colored light while illuminating. The function provided by OpenGL is `glMaterial`.

Besides, validness of illumination and material must be pointed out definitely in OpenGL. If illumination and material is not valid, and the color is simply only projected in to the current vertex and without the complex effect of normal vector, illumination and material superposed. The object with three-dimensional quality and sense of reality still can not be acquired, although the attributes of illumination and material are set up. The corresponding functions provided by OpenGL `glEnable` and `glDisable`, which are responsible for most set of function starting and closing. The concrete functions depend on the selection of parameters, `GL_LIGHTING` and `GL_COLOR_MATERIAL` are chose for illumination and material. The usage of the other functions can be found in MSDN [53].

### 5.2.5 Methods to display efficiently

OpenGL provides `glVertex` function to define the basis graphic primitive, but when we use a lot of continuous vertexes to display graphic primitive, a lot of time is wasted in the operating such as ascending vertex suffix and acquiring address. Then the display efficiency is lowered. In fact, OpenGL did a lot of work to improve the displaying efficiency, among which, Display list [54] and Vertex array [55] are more effective and can improve the efficiency favorably.

The common way to protract graphics is by Immediate mode, namely to protract while displaying with immediate function commands. The opposite one is Display list, which is composed of a group of function statements of pre-stored OpenGL for future calls. When we invoke this display list, function statements in the listed will be executed in turn. In general, the functions in display list are processed into the format suitable to graphics hardware, so the speed is superior to that of Immediate mode. `glNewList` and `glEndList` can be used to create display list. OpenGL function is stored between them and will be inserted into the display list; After setting up the display list, function `glCallList` is invoked to execute it, and the repeated executions of the same display list is permitted in the program. Immediate mode of the other functions can also be mixed with.

Vertex Array is the newly-added functions in OpenGL 1.5 edition, which put vertex data into array and use them directly in latter operations. Data block with same format can easily be latched down, the usage of function `glInterleavedArrays` can conveniently reset the vertex array. And the invoking of `glDrawArrays` can avoid the repeated usage of the same function, while the invoking of `glDrawElements` function can also reduce the repeated calculation of the same vertex. The series of methods can obviously improve the processing speed. But note that, to more memory may be took up in invoking these vertex array functions between `glBegin` and `glEnd`. So try to avoid using them in this case.

### 5.3 Data exchanging of application interface

3D laser scanning data after processing and reconstructing can be widely applied in manufacturing and process industries, and the reconstructed color data can be applied in many virtual reality technology such as online museums. The key of application is the creation of data interface, because different application fields have their own data formats, eg, STL format in reverse engineering, WRL format in virtual reality, DXF format in AutoCAD. The following task is to study some important file formats applied in industry so as to realize the exchanging of self-edit software and standard application data. The data output with smallest file format is developed for the complex application interface. That is, finite data type output is developed according to the primitive polygon used in software processing, such as point clouds data, meshes and free curved surfaces. It can satisfy application and meanwhile lower the complexity in software developing.

#### 5.3.1 ASC

ASC file is the common used data format in laser scanning data, which stores data in the order of scanning lines. ASC file format can be divided into ASCII code and binary code. The former is much simple and in wide application, shown as in figure 5.6(a). Scanning lines ends with the sign "S endscan + scanning line serial number n", the data before this is 3D data of the points on this scanning line; the file ends with the sign "\*\*\*end cloud\*\*". Most 3D processing software favor this data format; the scanning data in this

experiment is stored in this form. This software is capable to read this file format.

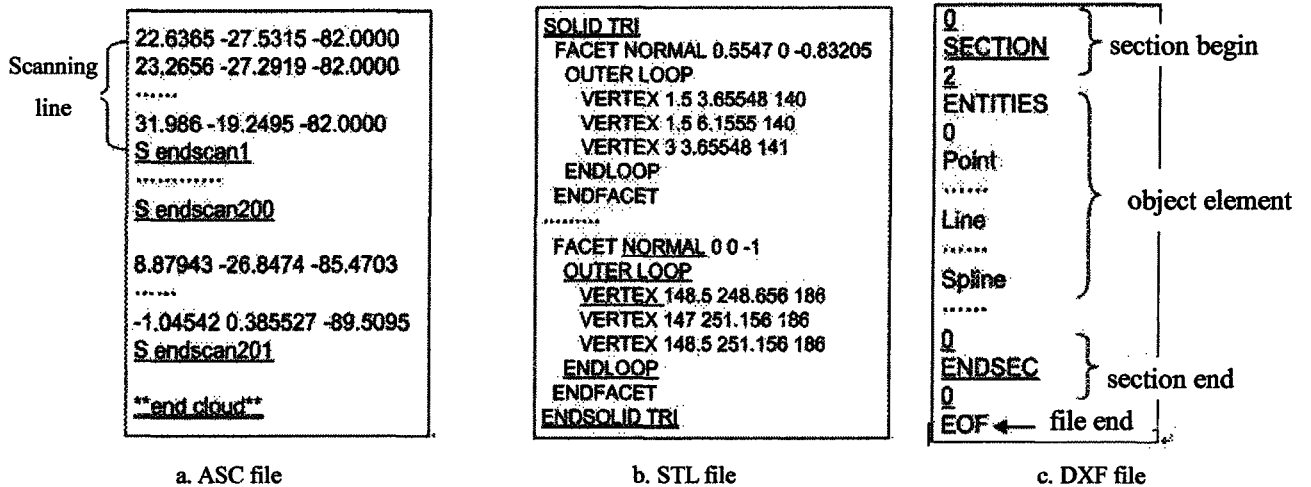


Figure 5.6 Examples for the format of application files

### 5.3.2 STL

STL (Stereolithography) file format is developed by 3D System cooperation, and now it has become the standard data transmission format for rapid prototyping industry. Up to now, almost all the rapid prototype system adopt this data format. And, all the main CAD/CAM software can directly output STL files. Its description for entity is unique.

STL file is acquired after triangular meshing of the three dimensional solid model. And its format contains ASCII code and binary code, the common used one is ASCII code. It is consisted of enormous triangular plans data, each triangular plan is described by a surface normal vector  $n$  and three vertexes denoted by three dimensional coordinates. One STL file can store many entities, signing as "SOLID + name of entities", data between "ENDSOLID + name of entities" is an entitative data, shown as in Figure 5.6(b). data of

small triangle surface is between signs“FACET”and“ENDFACET”, in which surface normal vector starts from NORMAL and vertex data starts from VERTEX and is put between “OUTER LOOP” and “ENDLOOP”.

### 5.3.3 IGES

IGES( Initial Graphics Exchange Specification )is the earliest and most widely used data exchanging criterion, which support curved surface, three-dimensional frame molding technology and solid geometry molding and boundary expressing molding technology. Its data structure is rather complex and overlaying most application scopes of CAD/CAM data exchanging.

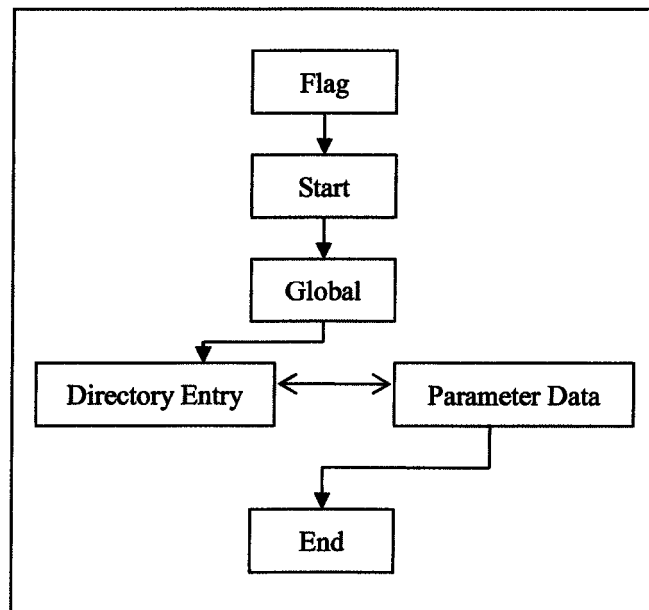


**Figure 5.7** IGES File Structure

The basic unit representing information in data exchanging files of IGES is element. Each element has one unique type number. In IGES criterion, five types of elements are

defined. They are curves/curved surface geometry element, solid constructing geometry element, boundary B-rep solid element, graphic denoting element and structure element. Abundant geometry types are defined in the type of fist element. Point clouds data, triangular mesh data and B-Spline solid data are favored. The solid type number of point is 116, of lines is 110(composing triangular mesh), of B-Spline is 126, of curved surface is 128; and the property setup of geometry graphs; and the type number of color definition is 314.

IGES is an ordinal file recording 80 characters with ASCII code, which contains 5-6 sections, shown as in Figure 5.7. Flag can be selected. Start provides some readable foreword explanation of the file; Global contains the original environment attribute information and file information of the description data. SOLID data information is stored in two important sections: Directory Entry and Parameter Data. And in Directory Entry, each element has one entry index, occupying two lines, and containing the type number of the element and other necessary description attributes value; while the Parameter Data contains the necessary geometry data value for describing elements, and corresponds to the attribute value of pointer and Directory Entry. Terminate Section regulates the total lines occupied by each section and orients for each section.

#### 5.3.4 DXF

DXF file format is a graphical data file format provided by the famous 3D design

software AutoCAD. Although it is not a criterion in itself, the wide application of AutoCAD has made it a factual data exchanging criterion. DXF is a text formatting with special ASCII code. One complete DXF file consists of 4 sections and 1 EOF, and the structure is rather complex, so it is very difficult to program an algorithm of output DXF. Auto CAD system permits to omit many items in DXF, and can still require a legal graph, so we can consider to create a smallest file format, namely only output ENTITIES section which is a necessary section in describing element when output DXF. Figure 5.6(c) show the outline structure of the created smallest file.

### 5.3.5 Examples of algorithm implementation

Output interface algorithm is provided for the above file format. In fact, if we understand the criterion requirement of the above interface file, the output of the data can be easily implemented. Among them, ASC file format is commonly used, and the software should not only realized output interface but also provided the corresponding input algorithm. Figure 5.8 represents the input algorithm of ASC file.

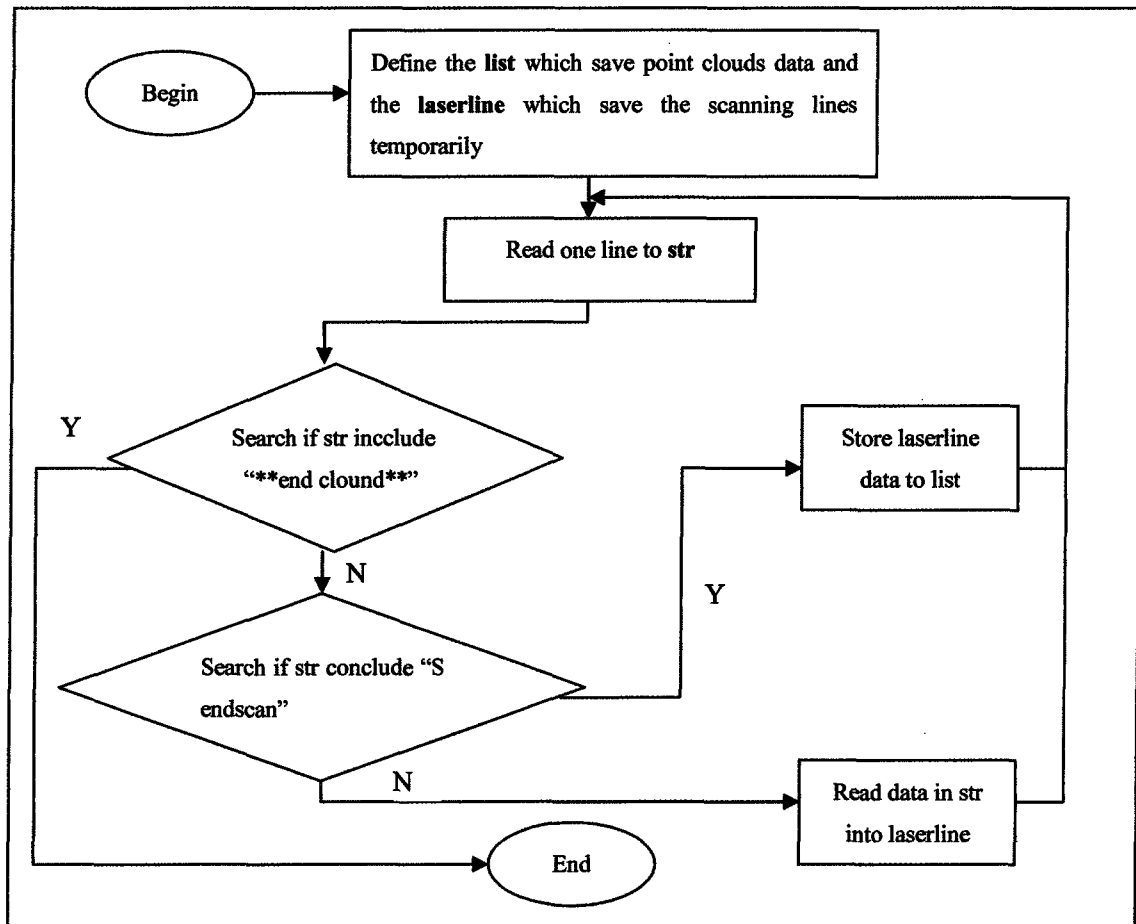


Figure 5.8 Procedure of reading and calculating ASC files

## 5.4 Chapter Summary

This chapter presented some common technologies in display and the common used data format of application interface which realized the data exchanging between the software processing results and the common 3D software (AutoCAD) and other software in industrial application (CNC).

**CHAPTER 6**

**INTRODUCTION OF SOFTWARE AND**

**PROCESSING EXAMPLES OF COLOR SCANNING DATA**

## **CHAPTER 6**

### **INTRODUCTION OF SOFTWARE AND PROCESSING EXAMPLES OF COLOR SCANNING DATA**

Based on the processing algorithms introduced in the previous chapters, this chapter will analyze two examples of the processing procedure of color laser scanning data.

The experiment is done in the conditions of the following.

Hardware requirements: at least Pentium 3 processor, at least 128M memory

Software environment: Windows operating system, Scan3D, OpenGL1.5 platform,  
3D Color Surf Ver1.0

The parameters of scanning system: field range : 50mm × 50mm ; scanning  
precision : 0.1mm.

#### **6.1 Introduction Of Software**

Now I will introduce the function of the 3D Color Surf software. Before using the software surface, we must use the scanning system software Scan3D just like figure 6.1 to get the original point clouds, with the dat as the scanning output file format.

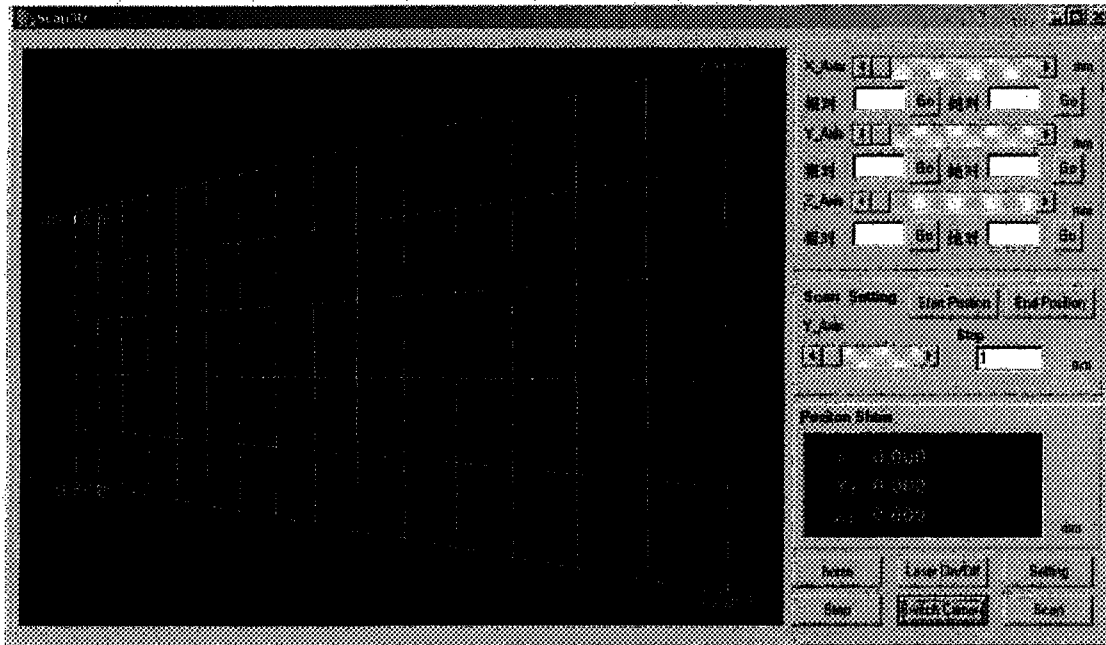


**Figure 6.1** Using scanning system to get the 3D data of object

Then we can use the surf software to process the data. Firstly we must select to open the different format files by the command “Open” from the menu “File”. Then the three-dimensional data can automatically be read into the memory and the time taking up dues to the file size.

After reading the three-dimensional data, the image will display on the screen just like figure 6.2. The function of the 3D Color Surf mainly include display setting, image input and output , data processing delete redundant data and mesh reconstruction etc.

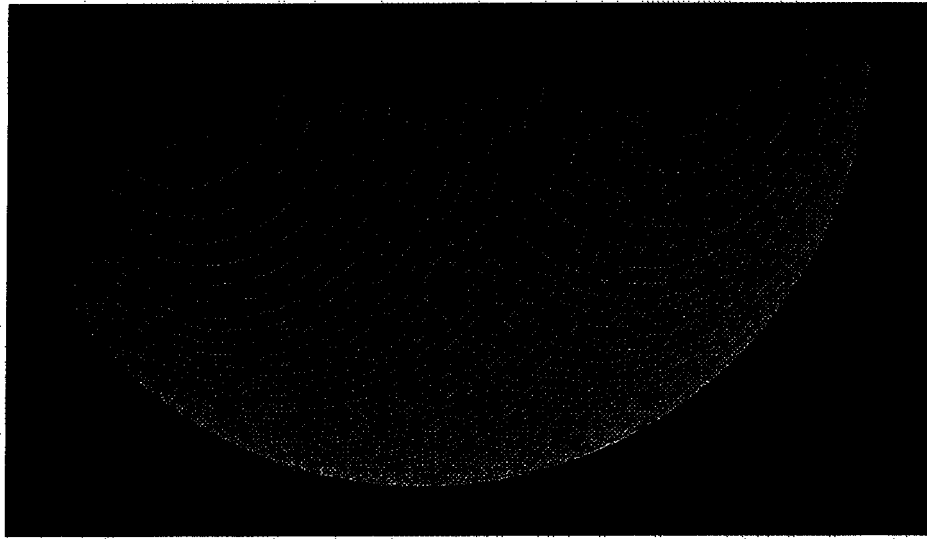


**Figure 6.2** Original point clouds of a ball surface

### 6.1.1 Display setting

We can use the command “Reference Setting” to set the display attribute. For example, the font proportion and color, the proportion of x, y and z, display size, display background color and coordinate scale etc. The coordinate scale is one important setting of these settings. It can set the video mode of 12 edges in the direction of axis x, axis y and axis z. The corresponding setting of axis x coordinate scale is as the following like figure 6.3.

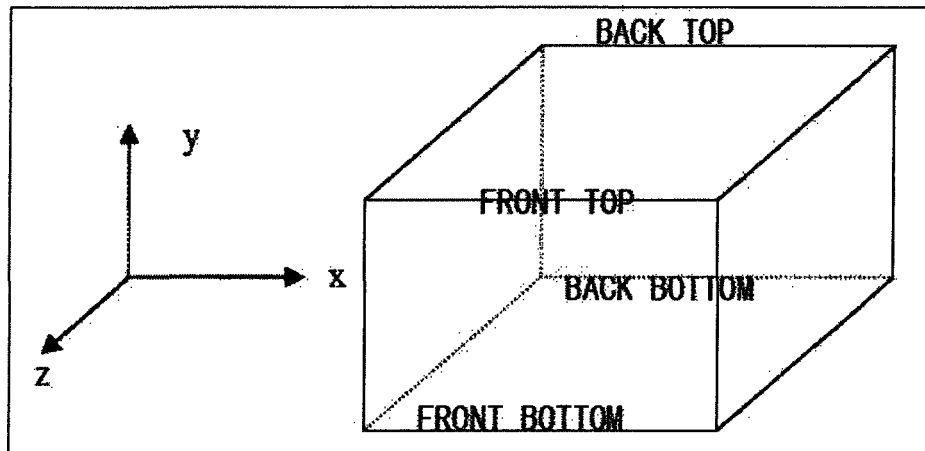


**Figure 6.3** Coordinate scale setting of axis x

### 6.1.2 Graph input and output

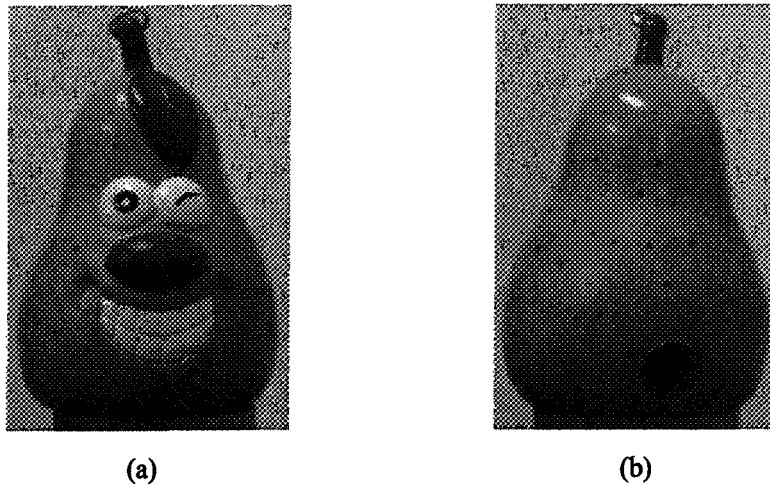
Three kind of graphic files with file extension .G3D, .JPG and .BMP can be opened directly and output by the software Surf. File extension .G3D contains the graph information and color information. It can be opened by the software and display on the screen. So do file extension .JPG and .BMP.

### 6.1.3 Data processing

The main functions of data processing include redundant points deleting, simplification and smoothing and mesh reconstruction etc. The functions can be executed by selecting the corresponding command from the menu "Data Processing". The detailed processing example will be introduced in the next section.

## 6.2 The Processing of Pencil-Sharpener Scanning Data

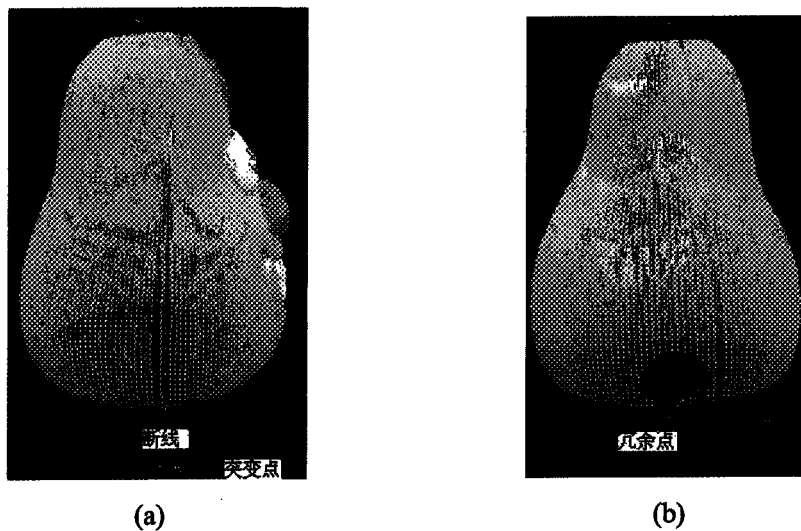
The data to be processed is pencil-sharpener scanning data. Figure 6.4 is the object picture of the pencil-sharpener. Its shell is made of soft material so it is suitable for laser to scan its appearances and outline. The way of data scanning is rotating scanning. Choose  $2^\circ$  as the steeper angle for its relative simple structure. The ultimate acquired number of point clouds data is 68961 points and the Bounding Box of point clouds data is the cube scope circled by  $(-12.30, -50.46, -112.30)$  and  $(36.0, 6.98, -65.13)$ , the core coordinate is  $(11.86, -21.74, -88.71)$ .



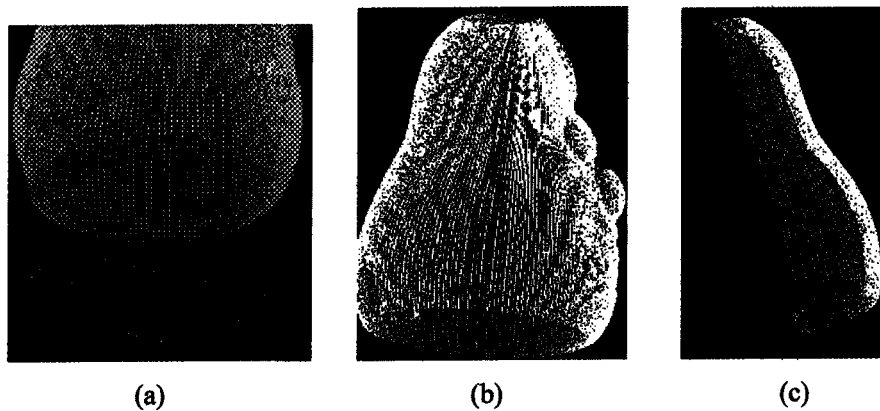
**Figure 6.4** The real image to be processed. (a) is the face view of image (b) is the back view of image

Figure 6.5 is the original data of scanning, in order to better represent the details of noise points, the points displayed in the diagram is the point clouds with twice enlargement. We can see the mutational points in the original data and some scanning broken lines with less data points influenced by environment. And there are some redundant points in the

hole at the back of the pencil sharpener. All these are to be deleted in pre-process. Figure 6.6 is the procedure. Here figure 6.6(a) mutational points deleting by selecting scanning broken lines. Figure 6.6(c) redundant points deleting which are difficult to operate in the inner point clouds after simple partition of point clouds data. Figure 6.8 is the result of noise deletion, which includes average smoothing effect.



**Figure 6.5** Original point clouds (68961 points ) (a)broken lines and mutation points  
(b) redundant points



**Figure 6.6** Process of noise deletion. (a) use method of frame-selected deletion to delete those noise data  
(b) use method of lines-selected deletion (c) use method of partition deletion

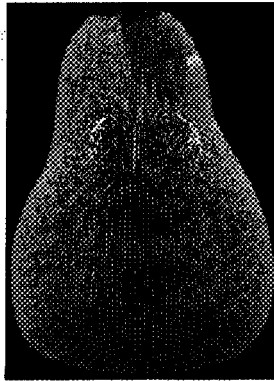


**Figure 6.7** Noise deletion result (68551points)

Figure 6.8 is point clouds diagram simplified by chord length algorithm. Figure 6.9(b) is the object displaying diagram of mesh model, and figure 6.9(a) is the chart of color model without point clouds data simplification; Figure 6.9(b) is the model with simplification but without color boundary restriction. Figure 6.9(c) displays the model of color boundary simplification. And here the time (unit: ms) consumed by mesh constructing and the number of meshes are listed in the brackets. From the reconstructed model, we can see that the model without color boundary restriction has some obvious distortion in color; while those data without simplification can more delicately display the attributes of objects but much more time will be consumed: And those reconstructed model with color boundary simplification has very vague distortion in shape and color, although it is not so detailed as the complete data. The time consumed and the number of reconstructed meshes is largely reduced, so it is a practical way to reconstruct color models.

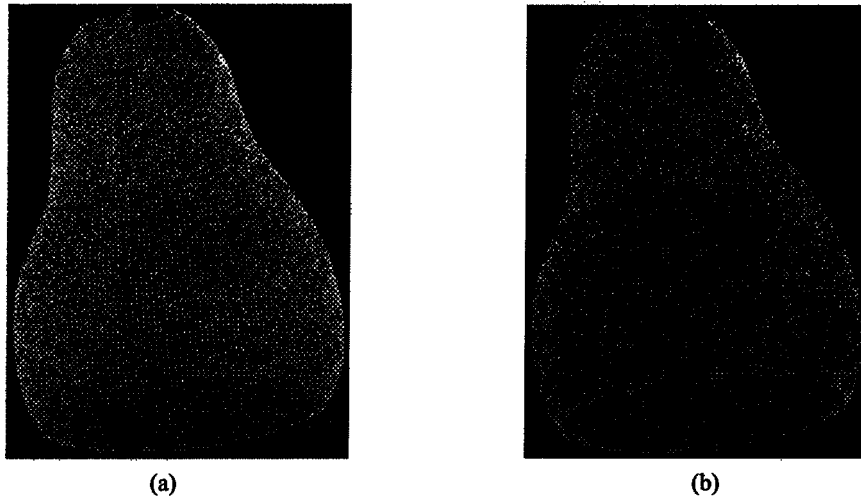


**Figure 6.8** Point clouds simplification (a) chord length ( length : 0.10mm , 21524points ) (b) chord length (length : 0.16mm , 11871points)

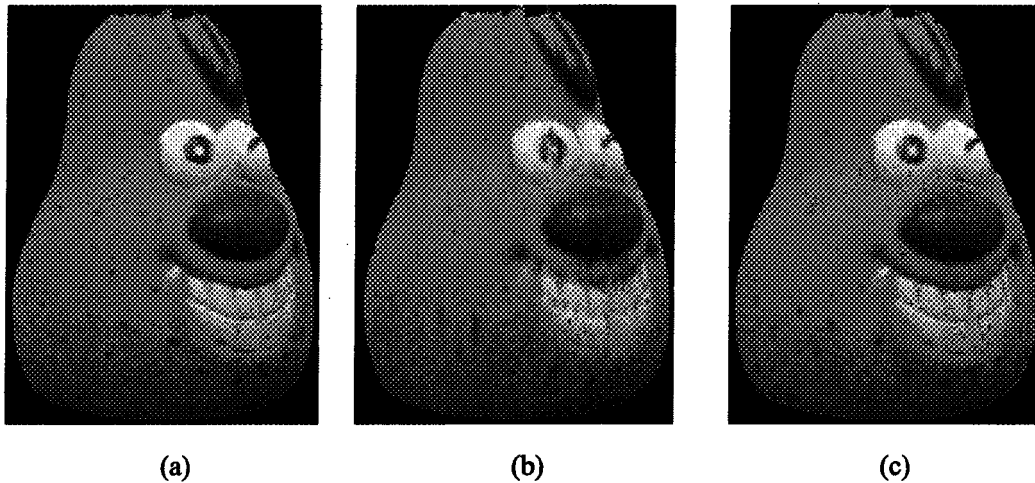


**Figure 6.9** Color model (a) complete data (136748meshes,68551points,time consuming 2406ms)  
 (b) non color boundary simplification (22422meshes,11388points,time consuming 624ms)  
 (c) color boundary simplification (23388meshes , 11871points , time consuming 668ms)

### 6.3 Chapter Summary

Based on the processing algorithms introduced in the previous chapters, this

chapter mainly analyzed an example of the processing procedure of color laser scanning data.

**CHAPTER 7**  
**CONCLUSION AND EXPECTATION**

## **CHAPTER 7**

### **CONCLUSION AND EXPECTATION**

This thesis is an initial study on the processing procedure of color 3D data based on software. It analyzes the arranging characteristics of laser scanning data, and the way to judge manually or automatically the redundant points and errors of point clouds data; and simplifies data with color boundary simplification algorithms while guarantees the original structure and color of the model; realizes the reconstruction of solid model of color objects by mesh construction and the interface processing of reverse engineering; realizes smoothing process of mesh model and implements the multi-resolution ratio displaying and thus solved the problem of different requirement of resolution ratio displaying due to the various speed in network application. At the same time, a processing software is designed to divide software with the support of OpenGL's key function of displaying technology and processing algorithm. The whole software is layer-structured and it realizes the separation of processing algorithm and data, and improves the feasibility of software editing and updating. Experiments are carried out with the software and it is proved that the algorithm adopted in the thesis is stable and practical in color 3D data processing.

Through the study of this subject, the proposed color 3D data processing procedure

and the corresponding algorithms are very prospective in the application of reverse engineering and virtual reality. But for the limitation of time and energy of the author, there are still some jobs needed to be continued and the algorithms realized still have some shortcomings, and which lowered the efficiency and practicality. The future study should be carried out from improving the current processing algorithms and making up for the processing functions. The following is a brief account of the key problems in the future study.

- 1 . Further study the algorithms of revising and interpolating the point clouds data to acquire more optimized data and improve the precision and visibility of reconstructed model.
- 2 . Realize the partition processing of the large data to simplify the complexity of processing on the different data blocks and to improve the processing speed of model reconstruction.
- 3 . Separate point clouds data and surface reconstructing them and realize the patching up of the curved surface data models.
- 4 . Enhance the edit function of reconstructed curves and surfaces to increase the application of the processing software; add more algorithms of stuffing scanning data flaws.
- 5 . Further optimize the design of code and software structure and improve the

processing efficiency ,reliability and feasibility of software;

- 6 . Add more data exchanging interfaces with virtual reality and enlarge the application in network technology of the software.

## BIBLIOGRAPHIES

- [1] Sun changku, Ye shenghua. Laser measurement technology. Tianjin University publishing house.2001
- [2] Niu Xiaobing, Research of the 3D outline measurement technology. Tianjin University.2003
- [3] Xu Zhiqing, Sun Changku, 3D reverse engineering technology. Chinese measurement publishing house. 2002
- [4] Alan C.Lin, Show-Yee Lin, Tse-Hao Fang. Automated sequence arrangement of 3D point data for surface fitting reverse engineering. Computer in Industry. 1998, 35: 149~173
- [5] D. Y. Chang, Y. M. Chang. A freedom surface modeling system based on laser scan data for reverse engineering. Int J Adv Manuf Technol. 2002. 20: 9~19
- [6] K. H. Lee, H. Woo, T. Suk. Data Reduction Methods for reverse engineering. Int J Adv Manuf Technol. 2001. 17: 735~743
- [7] K. H. Lee, H. Woo, T. Suk. Point Data Reduction using 3D Grids. Int J Adv Manuf Technol. 2001. 18: 201~210
- [8] H. Hoppe, T. DeRose, T. Duchamp, J. McDonald and W. Stuetzle. Surface reconstruction from unorganized points. Computer Graphics. 1992. 26(2): 71~76
- [9] L. A. Piegl, W. Tiller. Least-squares B-Spline curve approximation with arbitrary end derivatives. Engineering with Computers. 2000. 16: 109~116
- [10] Forsey DR, Bartels RH. Surface fitting with hierarchical splines. ACM transactions on Graphics. 1995. 14(2): 134~161
- [11] Lees. Wolberg, G. Shin SY. Scattered data interpolation with multilevel B-Splines. IEEE transaction on Visualization and Computer graphics. 1997. 3(3): 228~244
- [12] N. Amenta, M. Bern, M. Kamvysselis. A new Voronoi-based surface reconstruction algorithm. Proceeding of SIGGRAPH. 1998. 415~421
- [13] [13] L. Paul Chew. Guaranteed-Quality Mesh Generation for Curved Surfaces. In 9th Annual Symposium on Comp Geometry. 274~280
- [14] C. Bradley. Rapid prototyping models generated from machine vision data. Computers in Industry. 2001. 41: 159~173
- [15] M.S. Floater, M. Riemers. Meshless parameterization and surface reconstruction. Computer Aided Geometric Design. 2001. 18: 77~92
- [16] C.Zeng, M. Sonka. Local three dimensional shape preserving smoothing without shrinkage. Proceeding of international conference on image processing. 1997. Vol.1: 393~396
- [17] G.Taubin. Curve and surface smoothing without shrinkage. Proceeding of international conference on computer vision. 1995. 895~857
- [18] B.Wywill. An algorithm for polygon subdivision based on vertex normal. Proceeding of

- international conference on computer vision. 1997. 246: 3~12
- [19] P.Volino, N.M.Thalmann. The SPHERIGON: A simple polygon patch for smoothing quickly your polygonal meshes. Proceeding of international conference on computer vision. 1998. 72~78
- [20] William J. Schroeder, Jonathan A. Zarge. Decimation of triangle meshes. Proceeding of SIGGRAPH. 1992. In Computer Graphics, 26(2): 65~70
- [21] P. Verson, J.C. Leon. Static Polyhedron simplification using error measurements. Computer aided design. 1997. 29(4):287~298
- [22] Jarek Rossignac, Paul Borrel. Multi-resolution 3D approximations for rendering complex scenes. Modeling in Computer Graphics: Methods and Applications. 1993. 455~465
- [23] Michael Garland, Paul S. Heckbert. Surface simplification using quadric error metrics. Proceeding of SIGGRAPH. 1997. 209~216
- [24] Hugues Hoppe. Progressive meshes. Proceeding of SIGGRAPH. 1996. 99~108
- [25] Michael Garland, Paul S. Heckbert. Simplifying Surfaces with Color and Texture using Quadric Error Metrics. Proceedings of the conference on Visualization. 1998. In: IEEE Visualization. 263~269
- [26] H.K. Zhao, S. Osher, B. Merriman, M. Kang. Implicit and nonparametric shape reconstruction from unorganized data using a variational level set method. Computer Vision and Image Understanding. 2000. 80: 295~314
- [27] Wang Kai, Zhang Caiming. the Nerve Network Algorithm of the Free Curved Reconstruction.. the Journal of Computer-Aided Design and Graphics. 1998. 10(3): 193~199
- [28] Xiong Bangshu, Feng Yan etc. the research of curved surface's reconstruction. Engine science and technology. 22(3): 375~377
- [29] Milroy M J, Bradley C, Vickels G W. Segmentation of a wrap around model using an active contour. Computer-Aided Design. 1997. 29(4): 299~320
- [30] Yang M, Lee E. Segmentation of measured point data using a parametric quadric surface approximation. Computer-Aided Design. 1999. 31: 499~457
- [31] P. J. Besl, D. Mckay. A method for registration of 3-D Shapes. IEEE transactions on Pattern analysis and machine Intelligence. 1992. 14(2): 239~256
- [32] Xu Zhiqing, the Research of Portable Type 3D Laser Scanning System..Tianjin University. 2002
- [33] Pan Yunhe, the priciple, the means and the user of Computer graphics. Beijing higher education publishing house. 2001
- [34] Zheng Dehua. the Data Reduction of Point Cloud and Analysis of Reduction Effect. Engineering of Surveying and Mapping. Vol 15. No.4 ,Aug.,2006
- [35] Mark De Berg. Computational Geometry: Algorithms and Applications. Springer. February 2000
- [36] David F. Rogers, J. Alan Adams. Mathematical Elements for Computer Graphics. McGraw-Hill Science, 1989
- [37] Fan Guangzhao, Zhang ming etc. the technology and the application of reverse engineering.

Gao Li Books limited company.

- [38] Les. A. Piegl, Wayne Tiller. The NURBS Book (Monographs in Visual Communications). Springer Verlag. 1997
- [39] Zhang Wenjie, the higer definitional mearsurement and data processing research of the Free curved lines and surfaces. Tianjin University. 1995
- [40] Xu Shiliang. C programming algorithm assemble. Tsinghua University publishiing house. 1996
- [41] Jonathan Richard Shewchuk. Delaunay Refinement Algorithms for Triangular Mesh Generation. ACM transactions on Graphics, 2001
- [42] Peng Qunsheng, Bao Hujun etc. the beigining of Computer real figure algorithm. Science Publishing House, 1999
- [43] Sun Jiaguang, Yang Changgui, Computer graphics. Tsinghua Uuiversity publishing house. 1995
- [44] Ni Mingtian, Wu liangzhi, Computer graphics. Beijing University publishing house. 1999
- [45] Max McGuire, The Half-Edge data structure, <http://www.flipcode.com/>
- [46] Mathieu Desbrun, Mark Meyer, Peter Schröder, Alan Barr. Implicit Fairing of Irregular Meshes using Diffusion and Curvature Flow. Proceeding of SIGGRAPH. 1999. L.A., CA
- [47] G. Taubin. Geometric Signal Processing on Polygonal Meshes. ACM transactions on Graphics. 2000
- [48] Michael Garland, Paul S. Heckbert. Surface Simplification Using Quadric Error Metrics. Proceeding of SIGGRAPH. 1997. Annual Conference Series: 209~216
- [49] Wu Bin, Duan Haibo etc. OpenGL programming manul. Chinese electric power publishing house.2001
- [50] Michael Chen, S. Joy Mountfurd, Abigail Sellen. A Study in Interactive 3-D Rotation Using 2-D Control Devices. Computer Graphics. 1988. 22(4)
- [51] OpenGL Nehe Tutorials. <http://nehe.gamedev.net/>
- [52] Jackie Neider, Tom Davis, Mason Woo. OpenGL Programming Guide. Addison-Wesley Publishing Company, 1994
- [53] MSDN: Microsoft Software Development Network. <http://msdn.microsoft.com/>
- [54] <http://www.gameres.com/Resource/>
- [55] Fei Guangzheng, Lu Lidan etc. Visualization OpenGL programming design. Tsinghua University Publishing House. 2001
- [56] <http://www.gks.com/>
- [57] David F. Rogers and J. Alan Adams. Mathematical Elements for Computer Graphics, McGraw-Hill, pp.305-355.
- [58] Hong Jun, Ding Yuncheng, Cao Liang, Wu Dianliang. Data Cloud Direct Reduction in Reverse Engineering. Journal of xi'an JiaoTong Universtiy, Jul.2004.
- [59] <http://dev.gameres.com/Program/Abstract/Geometry.htm>
- [60] Dai Guangming, Wang MaoCai, Peng lei. Algorithm for smallest quadrangle encasing box of convex polygon. Journal of Huazhong University of Science and Technology(Nature Science), vol34. No.34,2006